



# A pursuit–evasion game between two identical differential drive robots

Luis Bravo<sup>a</sup>, Ubaldo Ruiz<sup>b,c,\*</sup>, Rafael Murrieta-Cid<sup>a</sup>

<sup>a</sup>*Centro de Investigación en Matemáticas, Guanajuato, Mexico*

<sup>b</sup>*Centro de Investigación Científica y de Educación Superior de Ensenada, Baja California, Mexico*

<sup>c</sup>*CONACYT, Ciudad de Mexico, Mexico*

Received 22 May 2019; received in revised form 5 February 2020; accepted 6 March 2020

Available online 20 March 2020

---

## Abstract

This paper addresses a pursuit–evasion problem between two identical Differential Drive Robots (DDRs). The pursuer wants to capture the evader in minimal time, while the evader wants to delay capture as much as possible. The game takes place in a Euclidean plane without obstacles. In this work, the motion primitives and time-optimal motion strategies for both players are presented. Based on the initial positions of the players, it is possible to solve the decision problem of determining the winner of the game. Simulations of the pursuit–evasion game showing the time-optimal motion primitives of the players are provided for both cases, when the pursuer wins and when the evader escapes.

© 2020 The Franklin Institute. Published by Elsevier Ltd. All rights reserved.

---

## 1. Introduction

This paper addresses a pursuit–evasion problem between two identical non-holonomic Differential Drive Robots (DDRs). A DDR has two wheels with independent motors that allow it to rotate in site. The pursuer wants to capture the evader in minimal time, while the evader wants to delay capture as much as possible. The game takes place in a Euclidean plane without

---

\* Corresponding author at: Centro de Investigación Científica y de Educación Superior de Ensenada, Baja California, Mexico.

*E-mail addresses:* [luixbravo@cimat.mx](mailto:luixbravo@cimat.mx) (L. Bravo), [uruiz@cicese.mx](mailto:uruiz@cicese.mx) (U. Ruiz), [murrieta@cimat.mx](mailto:murrieta@cimat.mx) (R. Murrieta-Cid).

obstacles. In this work, we find the motion primitives and time-optimal motion strategies for both players in open loop. The conditions defining the winner of the game are also provided.

This work presents a differential game; there are several previous works about differential games [1–5]. However, to the best of our knowledge, the previous works most closely related to the work presented in this paper are the following: [6–9]. In [6], the authors have addressed the problem of capturing an omnidirectional agent (OA) using a differential drive robot (DDR) in an obstacle-free environment. In [6], the authors have proposed a partition of the playing space into mutually disjoint regions where time-optimal motion strategies for the players are well established. The time-optimal motion strategies obtained in [6] are in Nash equilibrium, and the proposed strategies are in open loop. In [7], the authors presented a state feedback-based time-optimal motion policy based on the partition proposed in [6]. The state of the evader relative to the pursuer is estimated based on images using the one-dimensional trifocal tensor, and it is used to determine the corresponding motion strategy followed by the players. Later, in [9], the authors have shown that the location of the evader on the image can be directly used by the pursuer to define its motion strategy. That is, the pursuer can apply its motion strategy using the image without explicitly reconstructing the evader's position. From the Nash property, it follows that if the evader deviates from its maximum potential speed, then the capture time shall not increase for a pursuer that does not deviate from its Nash equilibrium motion strategy. However, it is not immediately clear how the pursuer could exploit that evader's deviation from its maximum potential speed, which might correspond to situations where the evader's capabilities may degrade with time, for example, battery depletion in an autonomous vehicle, or fatigue in an animal evader. This can be considered as a scenario of an evader in which the set of admissible controls varies with time. In [9] the authors also considered such a scenario.

In [8], the authors addressed the symmetric problem to the one presented in [6], in which the agents exchange roles. Thus, the OA is the pursuer and has as objective to capture the DDR in minimum time, and the DDR is the evader and wants to retard the capture as long as possible. Combining the results obtained in [8] and the ones in [6], the authors enable the agents to change the roles. Namely, the DDR is allowed to play as the pursuer, and the OA is allowed to play as the evader. This later analysis permits one to establish which is the winner role for each agent, based only on the initial position of the players and their maximum speed.

There are several practical applications of pursuit-evasion problems where the goal is capturing an agent in minimum time [1,2,6]. One example is a robotic system that wants to capture a malicious evader that can damage a human. Another example is a robotic system that wants to stop as fast as possible a driver that is violating the traffic rules putting in danger to other drivers.

For solving the problem addressed in this work, we use a known method in the literature called “the Isaacs methodology” [1]; however, there are two main novelties of our paper with respect to previous works [6–9]. The first difference is that in the game addressed in our work, both players have non-holonomic constraints while in differential games considering non-holonomic constraints like the ones in [6,8], the pursuer is a non-holonomic player, and the evader is omnidirectional (holonomic). That fundamental difference between this paper and previous works makes our problem harder to solve. Intuitively, a non-holonomic system has motion constraints; for instance, it cannot move instantaneously in all directions. More formally, the non-holonomic property of a system can be determined using the Frobenius Theorem [10]. The second difference is that the state-space has a higher dimension which also

makes more difficult obtaining and studying the solution. In our work, the state of the system can be expressed by the position and the orientation of the players as  $(x_p, y_p, \theta_p, x_e, y_e, \theta_e) \in \mathbb{R}^4 \times S^2$ . To simplify the problem, it can be stated in a reference frame that is fixed to the body of the pursuer. Thus, the state of the system can be expressed as  $\mathbf{x} = (x, y, \theta) \in \mathbb{R}^2 \times S^1$ . In previous works, as the Homicidal Chauffeur problem [1,2] or the work addressed in [6], the state-space has dimension 5, and it can be reduced to dimension 2 in a reference frame fixed to the pursuer, while in this work, initially the state-space has dimension 6, and it can be reduced to dimension 3 also defining a local reference frame attached to the pursuer. A crucial difference with previous classical works is that this increment in the state-space dimension has as a consequence that finding the loci of points called the barrier [1], defining the winner of the game, is considerably harder than in previous work [6–9]. In those works, the barrier was a curve in  $\mathbb{R}^2$ , while in this paper, we found that it is a surface embedded in  $\mathbb{R}^2 \times S^1$ , see Section 6. A higher dimension also makes it significantly harder to find the motion strategies for both players in all the playing space, see Section 7.

## 2. Related work and main contribution

The problem addressed in the paper is a pursuit-evasion game. In the area of control [1–3,5,9,11–13] and robotics [4,6,14–18] there has been a lot of interest in this kind of problems.

There are three main variants of pursuit-evasion games. One variant considers one or more pursuers that want to *find* one or more evaders in an environment with obstacles [14,15,17,18]. A survey of this kind of problem is presented in [19].

Other variant consists of *maintaining visibility of a moving evader* also in an environment with obstacles [4,16,20–23,25]. Game theory was proposed in [20] as a framework to formulate this problem.

In [4], the authors addressed the problem of maintaining visibility of the evader as a *game of degree* (i.e., the emphasis was over the optimization of a given criterion and not over the problem of deciding which player is the winner). The pursuer and the evader are omnidirectional (holonomic) systems. In [24], the problem of maintaining visibility of a moving omnidirectional evader with an omnidirectional pursuer was addressed as a *game of kind* (deciding which player wins). In [26], the authors addressed the problem of tracking (maintaining surveillance) of an omnidirectional mobile evader at *constant* distance with a Differential Drive Robot in an environment without obstacles. In [23] a robot has to track an unpredictable evader. An objective of O’Kane et al. [23] was to avoid the need for the pursuer to have detailed information about the evaders movements. A discrete-time fractional-order sliding scheme is proposed by Sun et al. [27] to drive the system. Such method could be used to tracking the predefined trajectories of the evader and the pursuer.

In a third variant of pursuit-evasion problems, the pursuer has as its goal to *capture the evader* [1,2,8], that is, move to a contact configuration, or closer than a given distance. *The work presented in this paper corresponds to this third variant.* A classic example of this kind of problems is the Homicidal Chauffeur problem [1,2]. In the homicidal chauffeur problem, a faster pursuer (w.r.t. the evader) has as its goal to get closer than a given constant distance (the capture condition) from a slower but more agile evader. The evader aims to avoid the capture condition. The pursuer is a nonholonomic system with a minimum turning radius, while the evader is an omnidirectional agent. The game takes place in the Euclidean plane without obstacles. Other related problems are the lady in the lake [12] and the lion and the man [11,28]. In the lady in the lake problem, there is a circular lake where a lady is

swimming with a maximum speed  $v_l$ , and there is a man that is in the side of the lake and runs along the shore with a maximum speed  $v_m$ ; the man cannot enter the lake, and the lady wants to leave the lake. The man runs with a larger speed than the one of the lady in the lake ( $v_l < v_m$ ). The man needs to capture the lady as soon as she reaches the shore since on land she runs faster than him. In the lion and the man problem, the players move in a circular arena; both players have the same motion capabilities, the lion wants to capture the man and the man wants to avoid the capture. In the same vein, in [29] the authors addressed a pursuit–evasion game in a graph called the cops and robbers game. The cops win the game if they can move to the robber’s vertex.

Only few works addressed the problem considering dynamics. In [5] the authors provided a dynamic formulation from a bio-inspired perspective. They characterized the dynamic properties of the system at two different levels: (1) the maneuvers and non-trivial escape of the evader and (2) the non-trivial escape zones for different ranges of the system parameters.

The case of multiple pursuers and evaders in the problem of capturing an evader has also been studied. The work in [13] addressed a class of multiplayer pursuit–evasion games with one superior evader, who moves faster than the pursuers. The authors studied the conditions under which the pursuers can capture the evader. In [30], the authors proposed a distributed algorithm for the cooperative pursuit of multiple evaders using multiple pursuers in a bounded, convex environment. In [31], the goal was to enclose and track a moving target by attaining a desired geometric formation around it.

There are many related works about pursuit–evasion both in the automatic control and robotics communities. However, to the best of our knowledge, the most closely related works to this paper are the following [6–9]. As it was mentioned above, the main difference of this work with the previous work in [6–9] is that in this paper both players are DDR, this implies that the dimension of the state space is larger than in the previous work above. That makes significantly harder to construct the representation of the barrier and find the motion strategies for both players in all the playing space. Here below we stress the contributions of this work that have not been presented before for the problem addressed in this paper.

- We found closed-form representations of the motion primitives and time-optimal strategies for the players. In the realistic space, the motion primitives are straight lines and rotations in place, see [Section 5](#).
- We exhibit the existence of cases where the evader wins (it avoids capture forever) which indicates that in the game addressed in this paper the barrier is closed, see [Section 6](#).
- Based on the initial configuration of the evader we can determine the winner of the game, see [Section 6](#).
- We provide insight about the motion strategies (controls of the players) in the playing space based on numerical analysis. In some of them both players merely move following straight lines but in others, one or the two players start rotating in place, and then they translate at maximum speed, see [Section 7](#).
- We provide simulations of the pursuit–evasion game showing the time-optimal motion primitives of the players both in a local reference frame defined with respect to the pursuer and in a global reference frame for cases in which either the pursuer or the evader wins, see [Section 8](#).

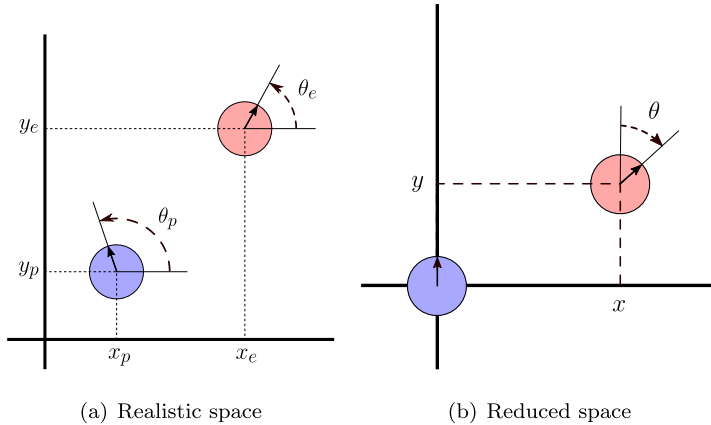


Fig. 1. (a) Shows a configuration of the players in the realistic space. (b) Shows the corresponding configuration using the pursuer’s position and its heading as the reference frame.

As quick reference for the remaining sections of the manuscript, we have included an appendix with two tables, one with the general notation and other with a list of acronyms defined in the paper.

### 3. Problem definition

Two identical Differential Drive Robots (DDRs) move on a plane without obstacles. One DDR (the pursuer) tries to capture the other DDR (the evader). The game is over when the distance between both is smaller than a critical value  $l_c$ . Both players have the same maximum bounded speed  $V^{\max}$ , and they can only change its motion direction at a rate that is inversely proportional to its translational speed [32]. This work considers a purely kinematic problem, and neglect any effects due to dynamic constraints (e.g., acceleration bounds). The pursuer wants to minimize the capture time  $t_f$  while the evader seeks to maximize it. The pursuer wins the game if it captures the evader in finite time while the evader wins if it can avoid capture forever. We find the conditions defining the winner of the game and the time-optimal motion strategies used by both players to achieve their goals.

## 4. Model

### 4.1. Realistic space

In this work, we assume that the two DDRs have the same motion capabilities, and without loss of generality both are equipped with unitary size wheels. In a global coordinate system (see Fig. 1(a)),  $(x_p, y_p, \theta_p)$  corresponds to the pose of the pursuer and  $(x_e, y_e, \theta_e)$  to the pose of the evader. That representation is usually known as the *realistic space* [1]. The state of the system can be expressed as  $(x_p, y_p, \theta_p, x_e, y_e, \theta_e) \in \mathbb{R}^4 \times S^2$ . The evolution of the system in

this coordinate system is described by the following motion equations

$$\begin{aligned} \dot{x}_p &= \left(\frac{u_1 + u_2}{2}\right) \cos \theta_p, \dot{y}_p = \left(\frac{u_1 + u_2}{2}\right) \sin \theta_p, \dot{\theta}_p = \left(\frac{u_2 - u_1}{2b}\right) \\ \dot{x}_e &= \left(\frac{v_1 + v_2}{2}\right) \cos \theta_e, \dot{y}_e = \left(\frac{v_1 + v_2}{2}\right) \sin \theta_e, \dot{\theta}_e = \left(\frac{v_2 - v_1}{2b}\right) \end{aligned} \tag{1}$$

where  $u_1, u_2 \in [-V^{max}, V^{max}]$  are the velocities of the left and the right wheel of the pursuer, respectively. Analogously,  $v_1, v_2 \in [-V^{max}, V^{max}]$  are the velocities of the left and the right wheel of the evader, respectively.  $b$  is the distance between the center of the robot and the wheel location. Note that since the wheels have unitary radius their translational and rotational speeds are equivalent. The heading angles of the players  $\theta_p$  and  $\theta_e$  are measured in counter-clockwise sense from the  $x$  positive axis (see Fig. 1(a)).

### 4.2. Reduced space

To simplify the analysis of the problem, we consider a space of reduced dimension. The problem can be stated in a reference frame that is fixed to the body of the pursuer (see Fig. 1(b)). The state of the system now can be expressed as  $\mathbf{x} = (x, y, \theta) \in \mathbb{R}^2 \times S^1$ . All the orientations in this reference frame are measured with respect to the positive  $y$ -axis in a clockwise sense. The coordinate transformation between the realistic and reduced spaces given by

$$\begin{aligned} x &= (x_e - x_p) \sin \theta_p - (y_e - y_p) \cos \theta_p \\ y &= (x_e - x_p) \cos \theta_p + (y_e - y_p) \sin \theta_p \\ \theta &= \theta_p - \theta_e \end{aligned} \tag{2}$$

Obtaining the time derivatives of Eq. (2), we obtain the following model of the kinematics in the pursuer-fixed reference frame

$$\begin{aligned} \dot{x} &= \left(\frac{u_2 - u_1}{2b}\right)y + \left(\frac{v_1 + v_2}{2}\right) \sin \theta \\ \dot{y} &= -\left(\frac{u_2 - u_1}{2b}\right)x - \left(\frac{u_1 + u_2}{2}\right) + \left(\frac{v_1 + v_2}{2}\right) \cos \theta \\ \dot{\theta} &= \left(\frac{u_2 - u_1}{2b}\right) - \left(\frac{v_2 - v_1}{2b}\right) \end{aligned} \tag{3}$$

This set of equations can be expressed in the form  $\dot{\mathbf{x}} = f(\mathbf{x}, u, v)$ , where  $u = (u_1, u_2) \in [-V^{max}, V^{max}] \times [-V^{max}, V^{max}]$ , and  $v = (v_1, v_2) \in [-V^{max}, V^{max}] \times [-V^{max}, V^{max}]$ . From now on, we will consider only the reduced space for this problem.

### 4.3. Hamiltonian

Following the approach in [1], we construct the Hamiltonian of the system. Recalling that

$$H(\mathbf{x}, \lambda, \mathbf{u}, \mathbf{v}) = \lambda^T \cdot f(\mathbf{x}, \mathbf{u}, \mathbf{v}) + L \tag{4}$$

and also that for problems of minimum time  $L = 1$ , we have

$$H = \lambda_x \left(\frac{u_2 - u_1}{2b}\right)y + \lambda_x \left(\frac{v_1 + v_2}{2}\right) \sin \theta - \lambda_y \left(\frac{u_2 - u_1}{2b}\right)x$$

$$-\lambda_y \left( \frac{u_1 + u_2}{2} \right) + \lambda_y \left( \frac{v_1 + v_2}{2} \right) \cos \theta + \lambda_\theta \left( \frac{u_2 - u_1}{2b} \right) - \lambda_\theta \left( \frac{v_2 - v_1}{2b} \right) + 1 \tag{5}$$

#### 4.4. Optimal controls

From [12], we know that along the optimal trajectories

$$\begin{aligned} \min_{\mathbf{u}} \max_{\mathbf{v}} H(\mathbf{x}, \lambda, \mathbf{u}, \mathbf{v}) &= 0 \\ u^* &= \arg \min_u H(\mathbf{x}, \lambda, \mathbf{u}, \mathbf{v}) \\ v^* &= \arg \max_v H(\mathbf{x}, \lambda, \mathbf{u}, \mathbf{v}) \end{aligned} \tag{6}$$

where  $u^*$  and  $v^*$  denote the optimal controls for the players. The pursuer’s goal is to minimize the capture time while the evader’s goal is to maximize it. From Eqs. (5) and (6) we have that

$$\begin{aligned} \min_{u_1, u_2} \max_{v_1, v_2} H &= \min_{u_1} \left[ u_1 \left( \frac{-\lambda_x}{2b} y + \frac{\lambda_y}{2b} x - \frac{\lambda_y}{2} - \frac{\lambda_\theta}{2b} \right) \right] + \min_{u_2} \left[ u_2 \left( \frac{\lambda_x}{2b} y - \frac{\lambda_y}{2b} x - \frac{\lambda_y}{2} + \frac{\lambda_\theta}{2b} \right) \right] \\ &+ \max_{v_1} \left[ v_1 \left( \frac{\lambda_x}{2} \sin \theta + \frac{\lambda_y}{2} \cos \theta + \frac{\lambda_\theta}{2b} \right) \right] + \max_{v_2} \left[ v_2 \left( \frac{\lambda_x}{2} \sin \theta + \frac{\lambda_y}{2} \cos \theta - \frac{\lambda_\theta}{2b} \right) \right] + 1 \end{aligned} \tag{7}$$

Thus,

$$\begin{aligned} u_1^* &= -V^{max} \operatorname{sgn} \left( -\frac{\lambda_x}{2b} y + \frac{\lambda_y}{2b} x - \frac{\lambda_y}{2} - \frac{\lambda_\theta}{2b} \right) \\ u_2^* &= -V^{max} \operatorname{sgn} \left( \frac{\lambda_x}{2b} y - \frac{\lambda_y}{2b} x - \frac{\lambda_y}{2} + \frac{\lambda_\theta}{2b} \right) \\ v_1^* &= V^{max} \operatorname{sgn} \left( \frac{\lambda_x}{2} \sin \theta + \frac{\lambda_y}{2} \cos \theta + \frac{\lambda_\theta}{2b} \right) \\ v_2^* &= V^{max} \operatorname{sgn} \left( \frac{\lambda_x}{2} \sin \theta + \frac{\lambda_y}{2} \cos \theta - \frac{\lambda_\theta}{2b} \right) \end{aligned} \tag{8}$$

#### 4.5. Adjoint equation

The adjoint equation is found by taking the partial derivative of the Hamiltonian with respect to the state variables. If  $t_f$  is the time of termination of the game, we define the retro-time as  $\tau = t_f - t$ . In this work, we denote the *retro-time derivative* of a variable  $x$  as  $\dot{\overset{\circ}{x}}$ . The adjoint equation in its retro-time form is

$$\dot{\overset{\circ}{\lambda}} = \frac{\partial}{\partial \mathbf{x}} H(\mathbf{x}, \lambda, u_1^*, u_2^*, v_1^*, v_2^*) \tag{9}$$

In this problem, we have that

$$\begin{aligned} \dot{\overset{\circ}{\lambda}}_x &= - \left( \frac{u_2^* - u_1^*}{2b} \right) \lambda_y, \dot{\overset{\circ}{\lambda}}_y = \left( \frac{u_2^* - u_1^*}{2b} \right) \lambda_x \\ \dot{\overset{\circ}{\lambda}}_\theta &= \left( \frac{v_1^* + v_2^*}{2} \right) (\lambda_x \cos \theta - \lambda_y \sin \theta) \end{aligned} \tag{10}$$

### 5. Optimal motion strategies

In this section, we will obtain the equilibrium strategies for the players. We follow the methodology presented in [1]. For more details, we refer the reader to [1,12].

#### 5.1. Primary solution

##### 5.1.1. Terminal surface

As it was described in [6], we need to compute the set of configurations where the pursuer guarantees termination (capture) regardless of the choice of controls of the evader. This set is known as the usable part (UP). For this problem, the pursuer captures the evader when the distance between both players is smaller than the capture distance  $l_c$  despite any opposition of the evader. In the reduced space, the terminal surface  $\zeta$  is a cylinder of radius  $l_c$  centered at the origin, and height  $2\pi$ . We can parametrized  $\zeta$  by two angles  $s_1$  and  $s_2$ .  $s_1$  is the angle between the evader’s position and the pursuer’s heading, and  $s_2$  is the angle between the headings of both players. Let  $l$  be the distance between the evader and the pursuer. In the reduced space, we can ensure capture when  $l = l_c$  and  $\dot{l} < 0$ . The UP of the game is given by

$$x = l_c \sin s_1, y = l_c \cos s_1, \theta = s_2, l^2 = x^2 + y^2, \min_{u_1, u_2} \max_{v_1, v_2} \dot{l} < 0 \tag{11}$$

Obtaining the time derivative for  $l$ , we have that:

$$\begin{aligned} \dot{l} = x\dot{x} + y\dot{y} = & x \left( \left( \frac{u_2 - u_1}{2b} \right) y + \left( \frac{v_1 + v_2}{2} \right) \sin \theta \right) \\ & + y \left( - \left( \frac{u_2 - u_1}{2b} \right) x - \left( \frac{u_1 + u_2}{2} \right) + \left( \frac{v_1 + v_2}{2} \right) \cos \theta \right) \end{aligned} \tag{12}$$

In the UP, from Eq. (11),

$$\begin{aligned} \dot{l} = & (\sin s_1 \sin s_2 + \cos s_1 \cos s_2) \left( \frac{v_1 + v_2}{2} \right) - \cos s_1 \left( \frac{u_1 + u_2}{2} \right) \\ = & \cos(s_1 - s_2) \left( \frac{v_1 + v_2}{2} \right) - \cos s_1 \left( \frac{u_1 + u_2}{2} \right) \end{aligned} \tag{13}$$

Applying the optimal controls for both players in the UP, we obtain

$$\min_{u_1, u_2} \max_{v_1, v_2} \dot{l} = -V^{max} |\cos s_1| + V^{max} |\cos(s_1 - s_2)| \tag{14}$$

Therefore, since the UP is given by

$$\min_{u_1, u_2} \max_{v_1, v_2} \dot{l} < 0$$

in this problem

$$UP = \{s_1, s_2 \mid |\cos s_1| > |\cos(s_1 - s_2)|\} \tag{15}$$

The boundary of the usable part (BUP) is defined by

$$\min_{u_1, u_2} \max_{v_1, v_2} \dot{l} = 0 \tag{16}$$

thus in this problem,

$$\text{BUP} = \{s_1, s_2 \mid |\cos s_1| = |\cos(s_1 - s_2)|\} \tag{17}$$

Note that  $|\cos s_1| = |\cos(s_1 - s_2)|$  when  $s_2 = 2s_1 + k\pi$  for all  $k \in \mathbb{Z}$ , or  $s_1 \in \mathbb{R}$  and  $s_2 = k\pi$ ,  $k \in \mathbb{Z}$ . We will refer to the set of configurations where  $s_2 = k\pi$  as surfaces of alignment (SoA), more details will be provided in Section 6.

5.1.2. Terminal conditions

From the UP, we have the values of  $x$ ,  $y$  and  $\theta$  at the terminal condition. We also need to establish the values of  $\lambda_x$ ,  $\lambda_y$  and  $\lambda_\theta$  on the UP of  $\zeta$ . From Eq. (11), we have that

$$\begin{aligned} \frac{\partial x}{\partial s_1} &= l_c \cos s_1, \quad \frac{\partial y}{\partial s_1} = -l_c \sin s_1, \quad \frac{\partial \theta}{\partial s_1} = 0 \\ \frac{\partial x}{\partial s_2} &= 0, \quad \frac{\partial y}{\partial s_2} = 0, \quad \frac{\partial \theta}{\partial s_2} = 1 \end{aligned} \tag{18}$$

Since  $\lambda(x) = 0$  on the UP, then  $\lambda_{s_1}$  and  $\lambda_{s_2}$  are given by

$$\begin{aligned} \lambda_{s_1} &= \frac{\partial \lambda}{\partial s_1} = \frac{\partial \lambda}{\partial x} \frac{\partial x}{\partial s_1} + \frac{\partial \lambda}{\partial y} \frac{\partial y}{\partial s_1} + \frac{\partial \lambda}{\partial \theta} \frac{\partial \theta}{\partial s_1} = \lambda_x \cos s_1 - \lambda_y \sin s_1 = 0 \\ \lambda_{s_2} &= \frac{\partial \lambda}{\partial s_2} = \frac{\partial \lambda}{\partial x} \frac{\partial x}{\partial s_2} + \frac{\partial \lambda}{\partial y} \frac{\partial y}{\partial s_2} + \frac{\partial \lambda}{\partial \theta} \frac{\partial \theta}{\partial s_2} = \lambda_\theta = 0 \end{aligned} \tag{19}$$

From Eq. (19), we obtain that

$$\lambda_x \cos s_1 = \lambda_y \sin s_1, \quad \lambda_\theta = 0 \tag{20}$$

Therefore

$$\lambda_x = \sin s_1, \quad \lambda_y = \cos s_1, \quad \lambda_\theta = 0 \tag{21}$$

5.1.3. Motion strategy at the end of the game

Substituting Eq. (21) into Eq. (8), we obtain the following values for the optimal controls of the pursuer

$$u_1^* = -V^{max} \text{sgn} \left( -\frac{\lambda_x}{2b} y + \frac{\lambda_y}{2b} x - \frac{\lambda_y}{2} - \frac{\lambda_\theta}{2b} \right) = -V^{max} \text{sgn} \left( -\frac{\cos s_1}{2} \right) \tag{22}$$

$$u_2^* = -V^{max} \text{sgn} \left( \frac{\lambda_x}{2b} y - \frac{\lambda_y}{2b} x - \frac{\lambda_y}{2} + \frac{\lambda_\theta}{2b} \right) = -V^{max} \text{sgn} \left( -\frac{\cos s_1}{2} \right) \tag{23}$$

The values of the optimal controls for the evader are given by

$$v_1^* = V^{max} \text{sgn} \left( \frac{\lambda_x}{2} \sin \theta + \frac{\lambda_y}{2} \cos \theta + \frac{\lambda_\theta}{2b} \right) = V^{max} \text{sgn} \left( \frac{\cos(s_1 - s_2)}{2} \right) \tag{24}$$

$$v_2^* = V^{max} \text{sgn} \left( \frac{\lambda_x}{2} \sin \theta + \frac{\lambda_y}{2} \cos \theta - \frac{\lambda_\theta}{2b} \right) = V^{max} \text{sgn} \left( \frac{\cos(s_1 - s_2)}{2} \right) \tag{25}$$

Note that  $u_1^* = u_2^*$  and  $v_1^* = v_2^*$ , thus both players end the game following a straight line motion at maximum speed. The motion direction of the players depends on the values of  $s_1$  and  $s_2$ .

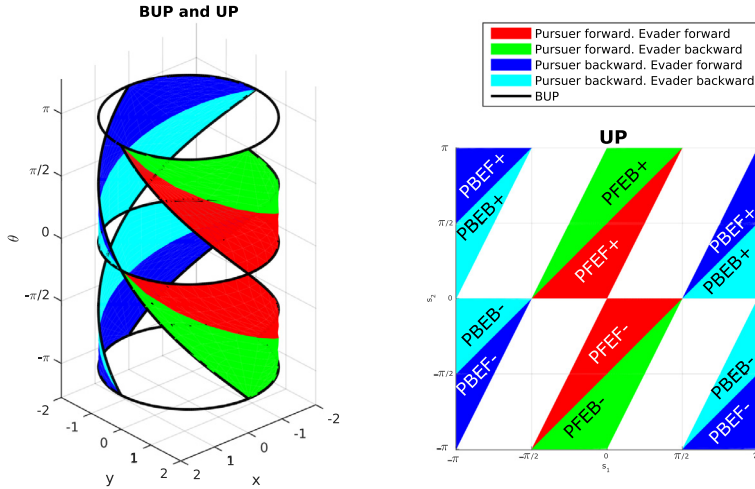
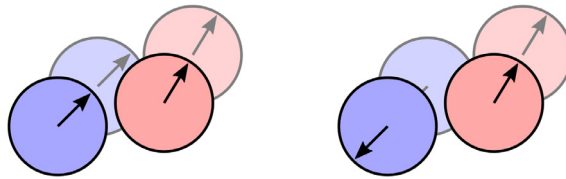


Fig. 2. Partition of the UP considering the motion direction of the players at the end of the game. For example, **PFEB-** means that the pursuer goes forward and the evader goes backward with  $s_2 < 0$  when the capture condition is reached.



(a) Both players move forward during the game (b) The pursuer moves backward during the game

Fig. 3. (a) Shows a case where capture is achieved with both players moving forward at maximum speed. The pursuer is represented by the blue disc and the evader by the red disc. In (b), the pursuer ends the game moving backward. Note that in both games, the initial and final positions are the same. (For interpretation of the references to color in this figure legend, the reader is referred to the web version of this article.)

### 5.1.4. Partition of the usable part considering the motion direction of the players

The UP can be parametrized by the angles  $s_1, s_2$  and the motion direction of the players at the end of the game. For simplicity, we focus our analysis for  $(s_1, s_2) \in [-\pi, \pi] \times [-\pi, \pi]$ . However, other parametrizations of the angles  $s_1, s_2$  are possible. We partition the UP into eight regions, shown in Fig. 2, labeled as PFEF+, PFEF-, PFEB+, PFEB-, PBEF+, PBEF-, PBEB+ and PBEB-. PF denotes that the pursuer is moving forward and PB that it is moving backward. Analogous, EF denotes that the evader is moving forward and EB that it is moving backward. The *plus* sign denotes that  $s_2 > 0$ , and the *minus* sign denotes that  $s_2 < 0$ . Notice that using Eqs. (22)–(25) we can tell at the end of the game, whether each player is moving forward or backward from the values of  $s_1$  and  $s_2$ .

Table 1  
Retro-time motion equations starting at the UP.

| $\dot{x}$              | $\dot{y}$                   | $\dot{\theta}$ | UP           |
|------------------------|-----------------------------|----------------|--------------|
| $-V^{max} \sin \theta$ | $V^{max} (1 - \cos \theta)$ | 0              | <b>PFEF±</b> |
| $V^{max} \sin \theta$  | $V^{max} (1 + \cos \theta)$ | 0              | <b>PFEB±</b> |

The system exhibits some symmetries for the angles  $s_1$  and  $s_2$ . Fig. 3 shows an example of these symmetries, we have two games with the same starting position but with different initial orientations for the pursuers. Those orientations differ from each other by a value of  $\pi$ . In this case, the controls for the players are only different by the sense of the motion direction for the pursuers. Note that in both games, the players end the game at the same position but with final orientations differing by a value of  $\pi$ . An analysis for the trajectories in regions PFEF+ and PFEB+ will be provided in this paper. This analysis can be extended to the remaining regions using analogous reasoning.

5.1.5. Solution of the adjoint equation

From the previous analysis, we know that at the end of the game the players follow a translation at maximum speed. Therefore Eq. (10) takes the form

$$\dot{\lambda}_x = 0, \dot{\lambda}_y = 0, \dot{\lambda}_\theta = \pm V^{max} (\lambda_x \cos \theta - \lambda_y \sin \theta) \tag{26}$$

where the sign of  $\dot{\lambda}_\theta$  depends on whether the evader is moving forward or backward at the end of the game. One can directly verify that

$$\lambda_x = \sin s_1, \lambda_y = \cos s_1, \lambda_\theta = \pm V^{max} \sin(s_1 - \theta) \tau \tag{27}$$

satisfies Eq. (26). This solution for the adjoint equation will be valid at the UP and as long as the players’ controls do not change, which corresponds to both players following a straight line in the realistic space. Later, we compute the retro-time instant when the players switch their controls.

5.1.6. Retro-time path equations

From Eq. (3), the retro-time version of the motion equations in the reduced space are

$$\begin{aligned} \dot{x} &= -\left(\frac{u_2 - u_1}{2b}\right)y - \left(\frac{v_1 + v_2}{2}\right) \sin \theta \\ \dot{y} &= \left(\frac{u_2 - u_1}{2b}\right)x + \left(\frac{u_1 + u_2}{2}\right) - \left(\frac{v_1 + v_2}{2}\right) \cos \theta \\ \dot{\theta} &= -\left(\frac{u_2 - u_1}{2b}\right) + \left(\frac{v_2 - v_1}{2b}\right) \end{aligned} \tag{28}$$

Substituting the optimal controls for each subregion of the UP, we obtain the retro-time motion equations starting at the UP shown in Table 1.

Integrating those motion equations with the initial conditions  $x = l_c \sin s_1, y = l_c \cos s_1$  and  $\theta = s_2$  we obtain the retro-time path equations in Table 2. Note that those equations give the motion of the system in the reduced space, in order to find the corresponding motion in the realistic space we need to apply the transformation given by Eq. (2).

Table 2  
Retro-time path equations starting at the UP for the subregions in Table 1.

| $x(\tau)$                               | $y(\tau)$                                    | $\theta(\tau)$ |
|---|--|----------------|
| $-\tau V^{max} \sin s_2 + l_c \sin s_1$ | $\tau V^{max} (1 - \cos s_2) + l_c \cos s_1$ | $s_2$          |
| $\tau V^{max} \sin s_2 + l_c \sin s_1$  | $\tau V^{max} (1 + \cos s_2) + l_c \cos s_1$ | $s_2$          |

### 5.2. Transition surface

The trajectories computed so far are valid as long as the players do not switch their controls. The place where a control variable abruptly changes its value is known as a *transition surface* (TS). In this subsection, we compute the retro-time instants at which the players switch their controls. First, we perform the analysis for the evader considering that it translates forward or backward at the end of the game, and later we extend our results for the pursuer.

#### 5.2.1. Evader translating forward

If the evader is moving forward, from Eq. (27) we have that  $\lambda_\theta = V^{max} \sin(s_1 - \theta)\tau$ . We know the control  $v_1$  is given by

$$v_1^* = V^{max} \operatorname{sgn}\left(\frac{\lambda_x}{2} \sin \theta + \frac{\lambda_y}{2} \cos \theta + \frac{\lambda_\theta}{2b}\right) \tag{29}$$

and it switches its sign when

$$0 = \frac{\lambda_x \sin s_2}{2} + \frac{\lambda_y \cos s_2}{2} + \frac{\lambda_\theta}{2b} \implies \frac{\sin s_1 \sin s_2}{2} + \frac{\cos s_1 \cos s_2}{2} + \frac{V^{max} \sin(s_1 - s_2)\tau}{2b} \tag{30}$$

thus

$$\tau = \frac{-b \cos(s_1 - s_2)}{V^{max} \sin(s_1 - s_2)} \tag{31}$$

The control  $v_2$  is given by

$$v_2^* = V^{max} \operatorname{sgn}\left(\frac{\lambda_x}{2} \sin \theta + \frac{\lambda_y}{2} \cos \theta - \frac{\lambda_\theta}{2b}\right) \tag{32}$$

and it switches its sign when

$$0 = \frac{\lambda_x \sin s_2}{2} + \frac{\lambda_y \cos s_2}{2} - \frac{\lambda_\theta}{2b} \implies \frac{\sin s_1 \sin s_2}{2} + \frac{\cos s_1 \cos s_2}{2} - \frac{V^{max} \sin(s_1 - s_2)\tau}{2b} \tag{33}$$

thus

$$\tau = \frac{b \cos(s_1 - s_2)}{V^{max} \sin(s_1 - s_2)} \tag{34}$$

#### 5.2.2. Evader translating backwards

If the evader is moving backwards, we have that  $\lambda_\theta = -V^{max} \sin(s_1 - \theta)\tau$ . In this case, the control  $v_1$  switches its sign at

$$\tau = \frac{b \cos(s_1 - s_2)}{V^{max} \sin(s_1 - s_2)} \tag{35}$$

The control  $v_2$  switches its sign at

$$\tau = \frac{-b \cos(s_1 - s_2)}{V^{max} \sin(s_1 - s_2)} \tag{36}$$

**5.2.3. Pursuer translating forward and evader translating forward**

From Eq. (27), we have that  $\lambda_\theta$  changes its sign according to the evader’s motion direction. In this case, we assume the evader is translating forward at the end of the game. Thus the next conditions are satisfied

$$\begin{aligned} x &= -\tau V^{max} \sin s_2 + l_c \sin s_1 \\ y &= \tau V^{max} (1 - \cos s_2) + l_c \cos s_1 \\ \lambda_\theta &= V^{max} \sin(s_1 - s_2)\tau \end{aligned} \tag{37}$$

note that

$$\begin{aligned} y\lambda_x - x\lambda_y + \lambda_\theta &= (\tau V^{max} (1 - \cos s_2) + l_c \cos s_1) \sin s_1 \\ &\quad - (-\tau V^{max} \sin s_2 + l_c \sin s_1) \cos s_1 + V^{max} \sin(s_1 - s_2)\tau \\ &= \tau V^{max} (\sin s_1 - \cos s_2 \sin s_1 + \sin s_2 \cos s_1 + \sin(s_1 - s_2)) \\ &= \tau V^{max} (\sin s_1 - \sin(s_1 - s_2) + \sin(s_1 - s_2)) = \tau V^{max} \sin s_1 \end{aligned} \tag{38}$$

The control  $u_1$  is given by

$$u_1^* = -V^{max} \operatorname{sgn}\left(-\frac{\lambda_x}{2b}y + \frac{\lambda_y}{2b}x - \frac{\lambda_y}{2} - \frac{\lambda_\theta}{2b}\right) \tag{39}$$

and it switches its sign when

$$0 = -y\lambda_x + x\lambda_y - \lambda_\theta - b\lambda_y = -\tau V^{max} \sin s_1 - b \cos s_1 \tag{40}$$

thus

$$\tau = \frac{-b \cos s_1}{V^{max} \sin s_1} \tag{41}$$

The control  $u_2$  is given by

$$u_2^* = -V^{max} \operatorname{sgn}\left(\frac{\lambda_x}{2b}y - \frac{\lambda_y}{2b}x - \frac{\lambda_y}{2} + \frac{\lambda_\theta}{2b}\right) \tag{42}$$

and it switches its sign when

$$0 = y\lambda_x - x\lambda_y + \lambda_\theta - b\lambda_y = \tau V^{max} \sin s_1 - b \cos s_1 \tag{43}$$

thus

$$\tau = \frac{b \cos s_1}{V^{max} \sin s_1} \tag{44}$$

**5.2.4. Pursuer translating forward and evader translating backward**

In this case, we assume the evader is translating forward at the end of the game. Following a similar analysis to the one in the previous subsection, we have that the control  $u_1$  switches its sign at

$$\tau = \frac{-b \cos s_1}{V^{max} \sin s_1} \tag{45}$$

and the control  $u_2$  switches its sign at

$$\tau = \frac{b \cos s_1}{V^{max} \sin s_1} \tag{46}$$

**Table 3**  
Switching controls for the evader at the TS depending on the region of the UP where the system begins.

| Control transition at $\tau_s$ | UP    | Rotation direction      |
|--------------------------------|-------|-------------------------|
| $v_1: + \rightarrow -$         | PFEF+ | Clockwise sense         |
| $v_1: - \rightarrow +$         | PFEB+ | Counter-clockwise sense |

**Table 4**  
Transition surface.

| $x(\tau_s)$   | $y(\tau_s)$   | $\theta(\tau_s)$ | UP    |
|---|---|------------------|-------|
| $\frac{b \cos(s_1 - s_2)}{\sin(s_1 - s_2)} \sin(s_2)$<br>$+ l_c \sin s_1$ | $-\frac{b \cos(s_1 - s_2)}{\sin(s_1 - s_2)} (1 - \cos s_2)$<br>$+ l_c \cos s_1$ | $s_2$            | PFEF+ |
| $\frac{b \cos(s_1 - s_2)}{\sin(s_1 - s_2)} \sin(s_2)$<br>$+ l_c \sin s_1$ | $\frac{b \cos(s_1 - s_2)}{\sin(s_1 - s_2)} (1 + \cos s_2)$<br>$+ l_c \cos s_1$  | $s_2$            | PFEB+ |

**Lemma 5.1.** *For retro-time trajectories starting at the UP, the evader changes its controls first than the pursuer at  $\tau_s = \left| \frac{b \cos(s_1 - s_2)}{V^{max} \sin(s_1 - s_2)} \right|$  and it starts a rotation in place at maximal rotational speed in the realistic space.*

**Proof.** From the previous subsection, we have that the pursuer switches its controls at  $\tau_s = \left| \frac{b \cos s_1}{V^{max} \sin s_1} \right|$  and the evader switches its controls at  $\tau_s = \left| \frac{b \cos(s_1 - s_2)}{V^{max} \sin(s_1 - s_2)} \right|$ . We know that if  $|\cos(a)| < |\cos(b)|$ , then  $|\sin(a)| > |\sin(b)|$ . Since  $s_1$  and  $s_2$  satisfy that  $|\cos(s_1 - s_2)| < |\cos(s_1)|$  at the UP (refer to Eq. (15)), and both players move following a straight line before one switches its controls, we have that  $|\sin(s_1 - s_2)| > |\sin(s_1)|$  which implies that  $\frac{1}{|\sin(s_1 - s_2)|} < \frac{1}{|\sin(s_1)|}$ . Multiplying both inequalities  $|\cos(s_1 - s_2)| < |\cos(s_1)|$  and  $\frac{1}{|\sin(s_1 - s_2)|} < \frac{1}{|\sin(s_1)|}$ , we get that  $\left| \frac{b \cos(s_1 - s_2)}{V^{max} \sin(s_1 - s_2)} \right| < \left| \frac{b \cos(s_1)}{V^{max} \sin(s_1)} \right|$ . Thus the evader switches its controls first than the pursuer.  $\square$

Considering the initial configurations in retro-time, we obtain the switching controls for the evader at  $\tau_s$  listed in Table 3.

From Lemma 5.1, and the equations in Table 2, we have that the transition surface is given by the equations in Table 4. It corresponds to the points in the reduced space where the evader switches its controls.

### 5.3. Retro-time path equations from the TS

Once the evader switches its controls and it starts rotating in place, we need to perform a new integration of the adjoint equation. Recalling that the pursuer continues translating at maximum speed, from Eq. (10), we have that

$$\dot{\lambda}_x = 0, \dot{\lambda}_y = 0, \dot{\lambda}_\theta = 0 \tag{47}$$

So,  $\lambda_x, \lambda_y,$  and  $\lambda_\theta$  are constant in retro-time. Taking as initial conditions the values of  $\lambda_x, \lambda_y,$  and  $\lambda_\theta$  at  $\tau_s$ , we have that

$$\lambda_x = \sin s_1, \lambda_y = \cos s_1 \tag{48}$$

And for  $\lambda_\theta$

|                      |       |
|----------------------|-------|
| $\lambda_\theta$     | UP    |
| $-b \cos(s_1 - s_2)$ | PFEF+ |
| $-b \cos(s_1 - s_2)$ | PFEB+ |

The retro-time motion equations after the evader switches its controls are

$$\dot{x} = 0, \dot{y} = \left( \frac{u_1 + u_2}{2} \right), \dot{\theta} = \left( \frac{v_2 - v_1}{2b} \right) \tag{49}$$

Integrating Eq. (49) taking as initial conditions the values of  $x(\tau_s)$ ,  $y(\tau_s)$ , and  $\theta(\tau_s)$  at TS, we obtain

|             |                                      |  |       |
|-------------|--------------------------------------|--|-------|
| $x(\tau)$   | $y(\tau)$                            | $\theta(\tau)$                           | UP    |
| $x(\tau_s)$ | $y(\tau_s) + V^{max}(\tau - \tau_s)$ | $s_2 + \frac{V^{max}}{b}(\tau - \tau_s)$ | PFEF+ |
| $x(\tau_s)$ | $y(\tau_s) + V^{max}(\tau - \tau_s)$ | $s_2 - \frac{V^{max}}{b}(\tau - \tau_s)$ | PFEB+ |

### 6. Game of kind

From [1], we have that the barrier separates the set of starting positions in those that result in capture and those that result in escape for the players. From starting points on the barrier, optimal behavior leads to a contact of the terminal surface without crossing it. The methodology that we have used in the calculation of the optimal strategies and their corresponding trajectories is also applied in the construction of the barrier. Whether or not the capture condition is achieved relies on whether or not the barrier divides the playing space into two parts.

#### 6.1. The barrier is closed

In this section, we show that the barrier is closed and it defines two regions in the playing space.

**Theorem 6.1.** *The barrier is closed and defines two regions in the playing space: one where the pursuer captures the evader, and another where the evader avoids capture forever.*

**Proof.** We prove this theorem by contradiction. Suppose the barrier is open, thus from [1], this means that the entire playing space is containing into one region, and the pursuer can capture the evader from any initial configuration. However, for this game, one can find different configurations where the pursuer is not able to capture the evader. Note that if both players are aligned, the pursuer can only maintain a constant distance because both players have the same speed. Also, assume the pursuer is heading directly to the evader, and the evader’s header is perpendicular to that orientation if the distance between both players is equal or greater than  $\frac{b\pi}{2}$ , then the evader can align its heading and it escapes maintaining a constant distance. Thus the assumption that the barrier is open and the playing space has only one region is false.  $\square$

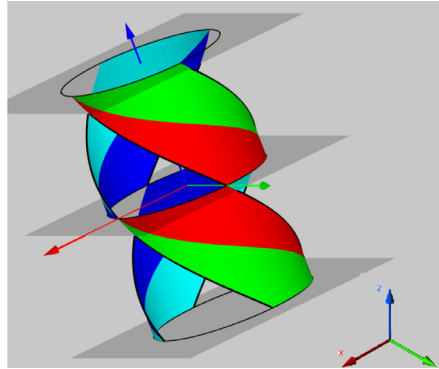


Fig. 4. The surfaces of alignment (SoA) correspond to those configurations where both players are heading in the same or opposite directions. They are represented by the dark gray planes. On those surfaces, the evader can always avoid capture regardless of the pursuer’s motion strategy.

### 6.2. Construction of the barrier

From Fig. 2, and the symmetries of the game, we have that the analysis of the retro-time trajectories starting at the BUP depends only on 3 different types of configurations. Those where  $s_2$  is of the form  $k\pi$  with  $k \in \mathbb{Z}$ ; those where  $s_2 = 2s_1$  and the trajectory starts from a configuration at the boundary of PFEF+; and those where  $s_2 = 2s_1 + \pi$  and the trajectory starts at the boundary of PFEB+.

It is important to note that for configurations starting at  $s_2 = k\pi$ , the players are heading in the same or opposite direction, and it is enough for the evader to keep moving following a straight line away from the pursuer to avoid the capture condition. The best strategy for the pursuer is to keep the initial distance following a straight line motion too. In this sense, we can define stationary surfaces containing configurations where the evader can guarantee to win regardless of its initial location in the reduced space. We will refer to these surfaces as *surfaces of alignment* (SoA) for the rest of the paper (see Fig. 4). Notice that those surfaces prevent trajectories starting from PFEF+, PFEB+, PBEB+, and PBEF+ to intersect trajectories from PFEF-, PFEB-, PBEB-, and PBEF-.

For the other two cases, the barrier is constructed integrating the adjoint equation (10) and the equations of motions (3) starting at the BUP. Similar to the case of the retro-time trajectories starting at the UP, the retro-time trajectories starting at the BUP correspond to straight lines where the players translate forward or backwards at maximum speed. Those trajectories are valid as long as the players do not switch their controls.

#### 6.2.1. Switching controls

Following a similar analysis to the one presented in Section 5.2, we found the time at which the players switch their controls. We define  $\tau_s^e$  as the transition time for the evader and  $\tau_s^p$  transition time for the pursuer. We have that

$$\begin{aligned} \tau_s^e &= \left| \frac{b \cos(s_1 - s_2)}{V^{max} \sin(s_1 - s_2)} \right| = \frac{b}{V^{max}} |\cot(s_1 - s_2)| \\ \tau_s^p &= \left| \frac{b \cos s_1}{V^{max} \sin s_1} \right| = \frac{b}{V^{max}} |\cot(s_1)| \end{aligned} \tag{50}$$

Table 5

Switching controls for the pursuer at the TS depending on the region of the BUP where the system begins.

| Control transition at $\tau_s^p$ | UP    | Rotation direction      |
|----------------------------------|-------|-------------------------|
| $u_2: + \rightarrow -$           | PFEF+ | Clockwise sense         |
| $u_1: + \rightarrow -$           | PFEB+ | Counter-clockwise sense |

Table 6

Controls of the players after the TS depending on the region of the BUP where the system begins.

| Control | from PFEF+ | from PFEB+ |
|---------|------------|------------|
| $u_1$   | $V^{max}$  | $-V^{max}$ |
| $u_2$   | $-V^{max}$ | $V^{max}$  |
| $v_1$   | $-V^{max}$ | $V^{max}$  |
| $v_2$   | $V^{max}$  | $-V^{max}$ |

For the case where  $s_2 = 2s_1 + k\pi$  for  $k \in \mathbb{Z}$ , we have

$$\tau_s^e = \frac{b}{V^{max}} |\cot(s_1 - s_2)| = \frac{b}{V^{max}} |\cot(s_1 - 2s_1 - k\pi)| = \frac{b}{V^{max}} |\cot(-s_1 - k\pi)| \tag{51}$$

Using the symmetry properties and periodicity of the *cotangent* function, we found that the times  $\tau_s^p$  and  $\tau_s^e$  are equal, i.e., the players switch their controls at the same time. Both players start a rotation in place. The controls for the evader have a similar pattern to the one shown in Table 3. Applying a similar reasoning for the pursuer, we obtain the pattern in Table 5.

6.2.2. Retro-time trajectory of the barrier after TS for  $s_2 = 2s_1$

The controls of the players after reaching the TS are shown in Table 6.

Using the controls defined for the retro-time trajectories starting from PFEF+, we can find the corresponding retro-time equations for the barrier.

$$\dot{x} = \frac{V^{max}}{b} y, \dot{y} = \frac{-V^{max}}{b} x, \dot{\theta} = \frac{2V^{max}}{b} \tag{52}$$

We can solve directly for  $\theta$  using as initial condition  $\theta(\tau_s) = s_2$ . So  $\theta(\tau) = \frac{2V^{max}}{b}(\tau - \tau_s) + s_2$  for  $\tau > \tau_s$ . For  $x$  and  $y$ , we have the follow initial conditions

$$\begin{aligned} x(\tau_s) &= -\left(\frac{b}{V^{max}} \cot(s_1)\right) \sin(s_2) + l_c \sin s_1 \\ &= -b \cot(s_1) \sin(2s_1) + l_c \sin s_1 = -2b \cos^2 s_1 + l_c \sin s_1 \\ y(\tau_s) &= -\left(\frac{b}{V^{max}} \cot(s_1)\right) (1 - \cos(s_2)) + l_c \cos s_1 = \\ &= b \cot(s_1) (1 - \cos(2s_1)) + l_c \cos s_1 = 2b \cos s_1 \sin s_1 + l_c \cos s_1 \end{aligned} \tag{53}$$

To solve Eq. (52), we compute its derivate and then we can solve the second order lineal differential equation given by  $\ddot{x} + \left(\frac{V^{max}}{b}\right)^2 x = 0$  and initial conditions  $x(\tau_s)$  and  $y(\tau_s)$ . We have

$$\begin{aligned} x(\tau) &= l_c \sin\left(s_1 - \cot(s_1) + \frac{V^{max}}{b} \tau\right) - 2b \cos(s_1) \cos\left(s_1 - \cot(s_1) + \frac{V^{max}}{b} \tau\right) \\ y(\tau) &= l_c \cos\left(s_1 - \cot(s_1) + \frac{V^{max}}{b} \tau\right) + 2b \cos(s_1) \sin\left(s_1 - \cot(s_1) + \frac{V^{max}}{b} \tau\right) \end{aligned} \tag{54}$$

6.2.3. *Retro-time trajectories from  $s_2 = 2s_1 + \pi$*

Using the controls defined for the retro-time trajectories starting from PFEB+ in Table 6, we can find the corresponding retro-time equations for the barrier.

$$\dot{x} = \frac{-V^{max}}{b}y, \dot{y} = \frac{V^{max}}{b}x, \dot{\theta} = \frac{-2V^{max}}{b} \tag{55}$$

We can solve directly for  $\theta$  using as initial condition  $\theta(\tau_s) = s_2$ . So  $\theta(\tau) = \frac{-2V^{max}}{b}(\tau - \tau_s) + s_2$  for  $\tau > \tau_s$ . For  $x$  and  $y$ , we have the follow initial conditions

$$\begin{aligned} x(\tau_s) &= \left( \frac{-b}{V^{max}} \cot(s_1) \right) \sin(s_2) + l_c \sin s_1 = \\ &= -b \cot(s_1) \sin(2s_1 + \pi) + l_c \sin s_1 = 2b \cos^2 s_1 + l_c \sin s_1 \\ y(\tau_s) &= \left( \frac{-b}{V^{max}} \cot(s_1) \right) (1 + \cos(s_2)) + l_c \cos s_1 = \\ &= -b \cot(s_1) (1 + \cos(2s_1 + \pi)) + l_c \cos s_1 = -2b \cos s_1 \sin s_1 + l_c \cos s_1 \end{aligned} \tag{56}$$

We can solve the second order lineal differential equation given by  $\ddot{x} + \left(\frac{V^{max}}{b}\right)^2 x = 0$  and initial conditions  $x(\tau_s)$  and  $y(\tau_s)$ . We obtain

$$\begin{aligned} x(\tau) &= l_c \sin \left( s_1 - \cot(s_1) - \frac{V^{max}}{b} \tau \right) + 2b \cos(s_1) \cos \left( s_1 - \cot(s_1) - \frac{V^{max}}{b} \tau \right) \\ y(\tau) &= l_c \cos \left( s_1 - \cot(s_1) - \frac{V^{max}}{b} \tau \right) - 2b \cos(s_1) \sin \left( s_1 - \cot(s_1) - \frac{V^{max}}{b} \tau \right) \end{aligned} \tag{57}$$

6.2.4. *Non-existence of a second switch of controls in the retro-time trajectories of the barrier*

We found that once both players switch their controls and they start rotating in place at maximum rotational speed, when they follow the retro-time trajectories of the barrier, the two players continue performing this motion strategy until they arrive to the SoA. To obtain this result, we perform a numerical analysis of the adjoint equation’s behavior after both players switch their controls. The optimal controls of the players directly depend on the adjoint equation.

Note that when the players are rotating in place at maximum rotational speed, the distance between them remains constant, and  $\theta$  increases or decreases if the retro-time trajectory started from PFEB+ or PFEF+, respectively. The time required to reach a SoA if both players continue rotating in place at maximum speed is denoted by  $\tau_{SoA}$ , and it is given by

$$\tau_{SoA} = \arg \min_{\tau > 0} \{ \theta(\tau) = k \cdot \pi \mid \forall k \in \mathbb{Z} \} \tag{58}$$

We can explicitly find  $\tau_{SoA}$  for retro-time trajectories starting from the BUP of PFEB+ or PFEF+. We have that

- $\tau_{SoA} = \frac{b}{2V^{max}}(\pi - s_2) + \tau_s$  for  $s_2$  at the BUP in PFEB+
- $\tau_{SoA} = \frac{b}{2V^{max}}s_2 + \tau_s$  for  $s_2$  at the BUP in PFEF+

We perform an analysis to detect if there is a change in the players’ controls after  $\tau_s$ , the time for the first switch of both players, and before  $\tau_{SoA}$ .

The next table shows the controls of the players before and after the switch when they travel the trajectories starting from the BUP

|                    | PFEF+  | PFEB+  |
|--------------------|--|--|
|                    | $u_1, u_2$   | $u_1, u_2$   |
| $\tau < \tau_s$    | $v_1, v_2$<br>$V^{max}, V^{max}$                                 | $v_1, v_2$<br>$V^{max}, V^{max}$                                   |
| $\tau \geq \tau_s$ | $V^{max}, V^{max}$<br>$V^{max}, -V^{max}$<br>$-V^{max}, V^{max}$ | $-V^{max}, -V^{max}$<br>$-V^{max}, V^{max}$<br>$V^{max}, -V^{max}$ |

Using the controls in the previous table and Eq. (10), we can find the expression of the adjoint equation after the first switch for the trajectory starting at the BUP of PFEF+, we have that

$$\dot{\lambda}_x = \frac{V^{max}}{b} \lambda_y, \dot{\lambda}_y = -\frac{V^{max}}{b} \lambda_x, \dot{\lambda}_\theta = 0 \tag{59}$$

Integrating the previous equations with the values of  $\lambda_x, \lambda_y$  and  $\lambda_\theta$  at  $t_s$  as initial conditions, we obtain that for  $\tau \geq \tau_s$

$$\begin{aligned} \lambda_x(\tau) &= \sin\left(s_1 + \frac{V^{max}}{b}(\tau - \tau_s)\right) \\ \lambda_y(\tau) &= \cos\left(s_1 + \frac{V^{max}}{b}(\tau - \tau_s)\right) \\ \lambda_\theta(\tau) &= b \cos\left(\frac{s_2}{2}\right) \end{aligned} \tag{60}$$

Substituting the previous equations into the optimal controls defined in Eq. (8), we have that its behavior depends on the sign of the following equations

$$\begin{aligned} f_{u_1}(\tau) &= -\lambda_x(\tau)y(\tau) + \lambda_y(\tau)x(\tau) - b\lambda_y(\tau) - \lambda_\theta(\tau) \\ f_{u_2}(\tau) &= \lambda_x(\tau)y(\tau) - \lambda_y(\tau)x(\tau) - b\lambda_y(\tau) + \lambda_\theta(\tau) \\ f_{v_1}(\tau) &= b\lambda_x(\tau) \sin(\theta(\tau)) + b\lambda_y(\tau) \cos(\theta(\tau)) + \lambda_\theta(\tau) \\ f_{v_2}(\tau) &= b\lambda_x(\tau) \sin(\theta(\tau)) + b\lambda_y(\tau) \cos(\theta(\tau)) - \lambda_\theta(\tau) \end{aligned} \tag{61}$$

We only focus our analysis on the interval  $\tau_s \leq \tau \leq \tau_{SoA}$ , i.e. after the first switch and before the game reaches the SoA. We define  $\tilde{\tau} = \tau - \tau_s$ . A plot of the last equations for the intervals  $0 \leq \tilde{\tau} \leq \tau_{SoA} - \tau_s$  and  $s_2 \in (0, \pi)$  over the BUP of PFEF+ is shown in Fig. 5.

A similar approach may be applied to the BUP of PFEB+. Notice that the functions do not cross the zero plane on the plots shown in Fig. 5 for the allowed values of  $\tau = \tau_s + \tilde{\tau}$ . Thus, we conclude that the trajectories end when they hit a SoA (see Fig. 6).

### 6.3. Characterization of the barrier

Now that we know how trajectories from the BUP behave, we would like to characterize the surface that is created by them. This characterization helps us to solve the game of kind, i.e., whether or not the pursuer/evader wins based on the initial configuration of the players. Notice that for a given value of  $s_2 \in (0, \pi)$ , we have two different values for  $s_1$  such that  $(s_1, s_2)$  is at the boundary of PFEF+ and PFEB+ (see Figs. 7 and 8). As it is shown in Fig. 7, we denote as  $\tilde{s}_1$  to the coordinate for  $s_1$  at the BUP that is next to PFEB+, and  $\hat{s}_1$  to the coordinate for  $s_1$  at the BUP that is next to PFEF+. Notice that each value is given by

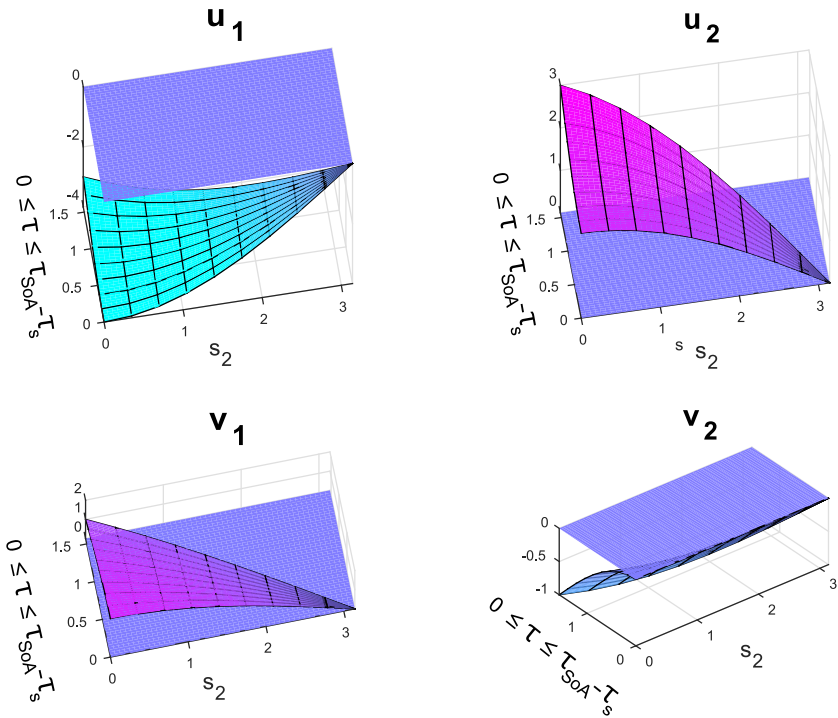


Fig. 5. Behavior of the functions that define the sign of each control after the first switch and before  $\tau_{SoA}$ . For the control  $u_1$ , the function  $f_{u_1}(\tau)$  increases its value but it never reaches zero (it does not change its sign). The same happens for  $v_2$ . For the control  $u_2$ , the function  $f_{u_2}(\tau)$  decreases its value but it does not reach zero before  $\tau_{SoA}$ , thus it does not change its sign. The control  $v_1$  shows a similar behavior. The previous results apply for any value  $s_2 \in [0, \pi]$ , and any  $\tilde{\tau} \in [0, \tau_{SoA} - \tau_s]$ .

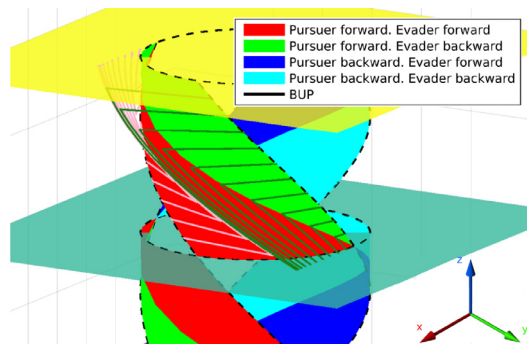


Fig. 6. The behavior of the BUP trajectories. Pink lines represent trajectories starting from the BUP of PFEF+, and dark green lines represent trajectories starting from the BUP of PFEB+. Turquoise and yellow planes correspond to the surface of alignment at  $s_2 = 0$  and  $s_2 = \pi$ , respectively. (For interpretation of the references to color in this figure legend, the reader is referred to the web version of this article.)

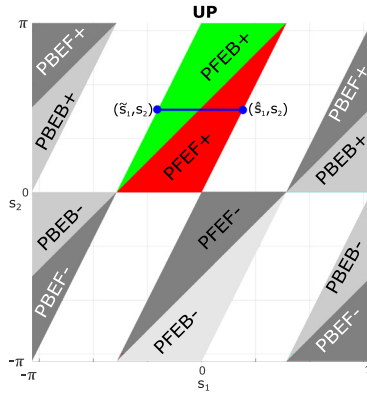


Fig. 7. Relation between  $s_2$  and its corresponding values for  $s_1$  at the BUP.

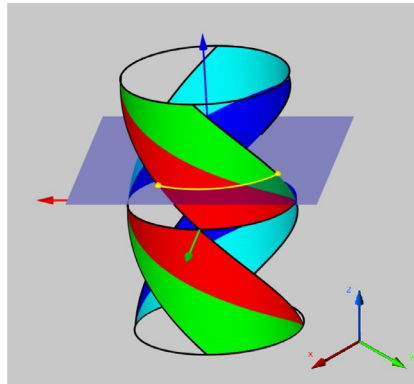


Fig. 8. Cross-section of the terminal surface at  $s_2 = 1$ . The yellow points are the points at the BUP for the PFEF+ and PFEF- regions. (For interpretation of the references to color in this figure legend, the reader is referred to the web version of this article.)

$$\tilde{s}_1 = \frac{s_2 - \pi}{2}, \hat{s}_1 = \frac{s_2}{2} \tag{62}$$

for a fixed value of  $s_2$ .

**Lemma 6.2.** Let  $(s_1, s_2)$  a point at the BUP(PFEF+), such that defines a trajectory  $(x(\tau), y(\tau), \theta(\tau)) : \tau \in [0, \infty) \rightarrow \mathbb{R}^3$  in retro-time using the optimal controls. Then, for a given time  $\hat{\tau}$ , we define the next points:

- $A = (x(\hat{\tau}), y(\hat{\tau}), \theta(\hat{\tau}))$ , the state of the game at retro-time  $\hat{\tau}$ .
- $B = \left( l_c \sin\left(\frac{\theta(\hat{\tau})}{2}\right), l_c \cos\left(\frac{\theta(\hat{\tau})}{2}\right), \theta(\hat{\tau}) \right)$ , the corresponding point at the BUP(PFEF+), for a level  $\theta(\hat{\tau})$ .
- $O = (0, 0, \theta(\hat{\tau}))$ , the origin of the game at level  $\theta(\hat{\tau})$ . The pursuer's position in the reduced space considering the evader's orientation.

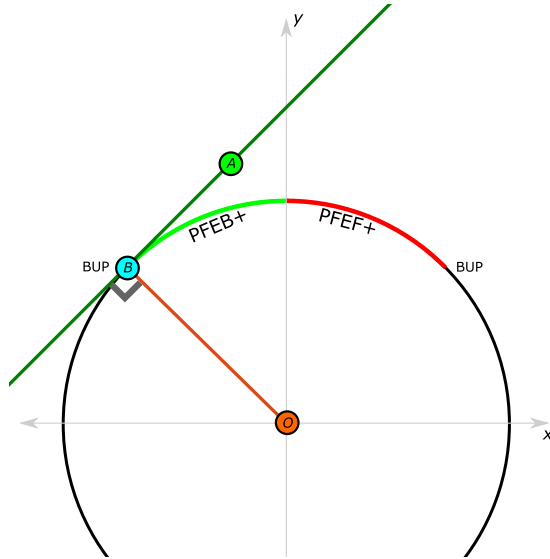


Fig. 9. The figure shows a slide of the reduced space at level  $s_2 = \frac{\pi}{2}$ . The dark green line represents the tangent line to the terminal surface at the BUP. The green, cyan and orange points are the ones defined by the proposition. (For interpretation of the references to color in this figure legend, the reader is referred to the web version of this article.)

The segments  $\overline{BA}$  and  $\overline{OB}$  are perpendicular. In other words, the trajectories starting from the BUP are tangent to the cross-section of the terminal surface at level  $\theta(\hat{\tau})$ .

**Proof.** We are going to use  $B$  as a reference point and check if both segments are perpendicular. We define the next two vectors

- $\vec{A} = A - B$
- $\vec{O} = O - B$

Suppose  $\hat{\tau} < \tau_s$ , we have that

$$\begin{aligned}
 x(\hat{\tau}) &= -\hat{\tau}V^{max} \sin(s_2) + l_c \sin(s_2/2) \\
 y(\hat{\tau}) &= \hat{\tau}V^{max} (1 - \cos(s_2)) + l_c \cos(s_2/2) \\
 \theta(\hat{\tau}) &= s_2
 \end{aligned}
 \tag{63}$$

Since  $s_1 = \frac{s_2}{2}$ , we obtain that

$$\begin{aligned}
 \vec{A} &= \left( x(\hat{\tau}) - l_c \sin\left(\frac{\theta(\hat{\tau})}{2}\right), y(\hat{\tau}) - l_c \cos\left(\frac{\theta(\hat{\tau})}{2}\right), \theta(\hat{\tau}) - \theta(\hat{\tau}) \right) \\
 &= \left( -\hat{\tau}V^{max} \sin(s_2), \hat{\tau}V^{max} (1 - \cos(s_2)), 0 \right) \\
 \vec{O} &= \left( -l_c \sin\left(\frac{\theta(\hat{\tau})}{2}\right), -l_c \cos\left(\frac{\theta(\hat{\tau})}{2}\right), \theta(\hat{\tau}) - \theta(\hat{\tau}) \right) \\
 &= \left( -l_c \sin\left(\frac{s_2}{2}\right), -l_c \cos\left(\frac{s_2}{2}\right), 0 \right)
 \end{aligned}
 \tag{64}$$

And the dot product is given by

$$\begin{aligned} \vec{A} \cdot \vec{O} &= (-\hat{\tau}V^{max} \sin(s_2))\left(-l_c \sin\left(\frac{s_2}{2}\right)\right) + (\hat{\tau}V^{max}(1 - \cos(s_2)))\left(-l_c \cos\left(\frac{s_2}{2}\right)\right) \\ &= \hat{\tau}V^{max}l_c(-\cos(s_2 - s_2/2) + \cos(s_2/2)) = 0 \end{aligned} \tag{65}$$

Thus, can we conclude that  $\overline{BA}$  and  $\overline{OB}$  are perpendicular when  $\hat{\tau} \leq \tau_s$ . Now, suppose  $\hat{\tau} \geq \tau_s$ , from Eq. (54), the state of the game is given by

$$\begin{aligned} x(\hat{\tau}) &= l_c \sin \Theta - 2b \cos(s_2/2) \cos \Theta \\ y(\hat{\tau}) &= l_c \cos \Theta + 2b \cos(s_2/2) \sin \Theta \\ \theta(\hat{\tau}) &= s_2 + \frac{2V^{max}}{b}(\hat{\tau} - \tau_s) = s_2 + \frac{2V^{max}}{b}\left(\hat{\tau} - \frac{b}{V^{max}} \cot(s_2/2)\right) \\ &= s_2 + \frac{2V^{max}}{b}\hat{\tau} - 2 \cot(s_2/2) = s_2 + \frac{2V^{max}}{b}\tau - 2 \cot(s_2/2) \\ &= 2\left(s_2/2 - \cot(s_2/2) + \frac{V^{max}}{b}\hat{\tau}\right) = 2\Theta \end{aligned} \tag{66}$$

where  $\Theta = s_2/2 - \cot(s_2/2) + \frac{V^{max}}{b}\hat{\tau}$ . Translating the origin to the intersection of both lines

$$\begin{aligned} \vec{A} &= \left(x(\hat{\tau}) - l_c \sin\left(\frac{\theta(\hat{\tau})}{2}\right), y(\hat{\tau}) - l_c \cos\left(\frac{\theta(\hat{\tau})}{2}\right), \theta(\hat{\tau}) - \theta(\hat{\tau})\right) \\ &= (-2b \cos(s_2/2) \cos \Theta, 2b \cos(s_2/2) \sin \Theta, 0) \end{aligned} \tag{67}$$

and

$$\vec{O} = \left(-l_c \sin\left(\frac{\theta(\hat{\tau})}{2}\right), -l_c \cos\left(\frac{\theta(\hat{\tau})}{2}\right), \theta(\hat{\tau}) - \theta(\hat{\tau})\right) = (-l_c \sin \Theta, -l_c \cos \Theta, 0) \tag{68}$$

The dot product is given by

$$\vec{A} \cdot \vec{O} = (-2b \cos(s_2/2) \cos \Theta)(-l_c \sin \Theta) + (2b \cos(s_2/2) \sin \Theta)(-l_c \cos \Theta) = 0 \tag{69}$$

And we have that  $\overline{BA}$  and  $\overline{OB}$  are perpendicular when  $\hat{\tau} \geq \tau_s$ .  $\square$

If we take a cross-section of the playing space in the reduced space, we can see that the barrier looks like a triangle with tangents to the circle defined by the cross-section over the terminal surface (see Fig. 10).

Numerically, we have observed that no trajectory from the BUP reaches the point *C* shown in Fig. 10. Hence, we are going to define the controls in those configurations analyzing some cases. We ignore the case when the pursuer goes backward since that control gives an advantage to the evader. In simulations, we found that if the evader moves forwards or backward, and the pursuer goes forwards, then the trajectory in the reduced space moves along the barrier in the same cross-section ( $\theta$  does not change when both move following a straight line).

Additionally, if the evader rotates, there is a sense of rotation in which the evader’s position in the reduced space can be detached of the barrier even though the pursuer chooses to move forward. In this case, the best thing that the pursuer can do is also to perform a rotation in place. Those rotations take the game to a configuration where both players are heading in the same direction, i.e., a surface of alignment. As we know, these configurations correspond to escape for the evader. In conclusion, the point *C* is part of the barrier.

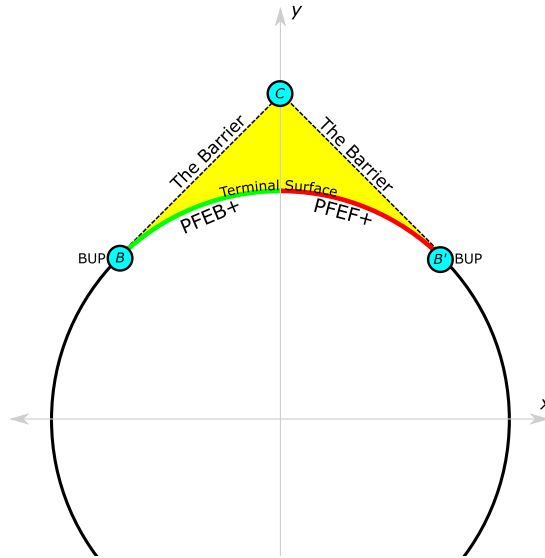


Fig. 10. Cross-section at  $s_2 = \frac{\pi}{2}$ , seen from top. In this case, the values for  $s_1$  at the BUP are  $\pi/4$  and  $-\pi/4$ .

**Corollary 6.3.** Let  $s_2 \in [0, \pi]$  define a cross-section of the playing space over  $\theta$  in the reduced space. Define the points  $B$ ,  $B'$ , and  $C$  as:

$$\begin{aligned}
 B &= \left( l_c \sin \left( \frac{s_2}{2} \right), l_c \cos \left( \frac{s_2}{2} \right), s_2 \right) \\
 B' &= \left( l_c \sin \left( \frac{s_2 - \pi}{2} \right), l_c \cos \left( \frac{s_2 - \pi}{2} \right), s_2 \right) \\
 C &= \left( l_c \left( \sin \left( \frac{s_2}{2} \right) + \sin \left( \frac{s_2 - \pi}{2} \right) \right), l_c \left( \cos \left( \frac{s_2}{2} \right) + \cos \left( \frac{s_2 - \pi}{2} \right) \right), s_2 \right)
 \end{aligned} \tag{70}$$

Then, the barrier, for PFEF+ and PFEB+ is defined by the cross-section of the terminal surface at  $s_2$ , and the segments  $BC$  and  $B'C$  (see Fig. 10).

Using the previous results, we can determine if the pursuer or the evader wins the game. This decision is made based on whether the initial configuration of the players for a given value of  $s_2$  is inside or outside of the yellow region defined by the barrier shown in Fig. 10. This idea is formalized in the following theorem

**Theorem 6.4.** Based only on the initial position of the evader in the reduced space it is possible to determine the winner of the game.

**Proof.** By Lemma 6.2 we know that the barrier is characterized by the segments  $\overline{BC}$  and  $\overline{B'C}$ . By the definition of the barrier [1], if the evader is inside the region defined by those segments and the UP, then the pursuer wins. Otherwise, the evader wins.  $\square$

### 7. Partitioning the playing space and analysis of singular surfaces

In this section, we would like to determine whether or not the controls that the players must apply are defined for the entire region of the playing space where the pursuer wins. The



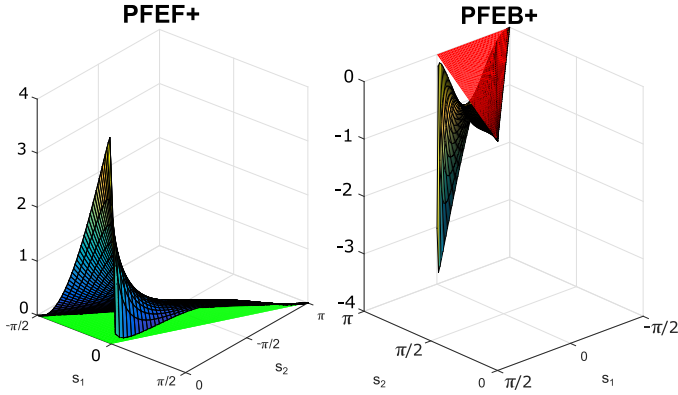


Fig. 12. Orientation analysis of trajectories at the first switch of controls with respect to the magenta segment defined in Fig. 11.

$$\begin{aligned}
 E &= \left( l_c \left( \sin \left( \frac{\theta}{2} \right) + \sin \left( \frac{\theta - \pi}{2} \right) \right), l_c \left( \cos \left( \frac{\theta}{2} \right) + \cos \left( \frac{\theta - \pi}{2} \right) \right), \theta \right) \\
 &= \left( l_c \left( \sin \left( \frac{\theta}{2} \right) - \cos \left( \frac{\theta}{2} \right) \right), l_c \left( \cos \left( \frac{\theta}{2} \right) + \sin \left( \frac{\theta}{2} \right) \right), \theta \right) \\
 F &= (x(\tau_s), y(\tau_s), \theta)
 \end{aligned} \tag{71}$$

where  $F$  is the evader’s position at the switching time  $\tau_s$ .  $F$  depends on  $s_1$  and  $s_2$ , the parameters of the evader’s position when capture is achieved. That is the partition of the UP where the trajectory is defined. We use the  $(x, y)$ -projection only since the third coordinate is the same. The function that defines the side where  $F$  is located with respect to the  $\overline{DE}$  segment (see Fig. 11) is given by the sign of

$$\begin{cases}
 >0 & \text{Points are in clockwise sense} \\
 = 0 & \text{Points are collinear} \\
 < 0 & \text{Points are in counter-clockwise sense}
 \end{cases} \tag{72}$$

the *clock-wise test* for three points.

As it was mentioned, our analysis is numerical. Fig. 12 shows the location of the third point  $F$  with respect to the segment  $\overline{DE}$  projected over the  $(x, y)$ -plane. Eq. (72) maintains its sign for PFEF+ and PFEB+. That is, trajectories from PFEF+ and PFEB+ do not cross the magenta line shown in Fig. 11. Then, we conclude that there is not a singular surface before the first switch of controls.

### 7.2. Singular surfaces after the first switch of controls

We continue our analysis of the trajectories after the first switch of controls. We want to find whether there is another transition surface (a second switch of controls), or whether trajectories intersect with each other (another kind of singular surface).

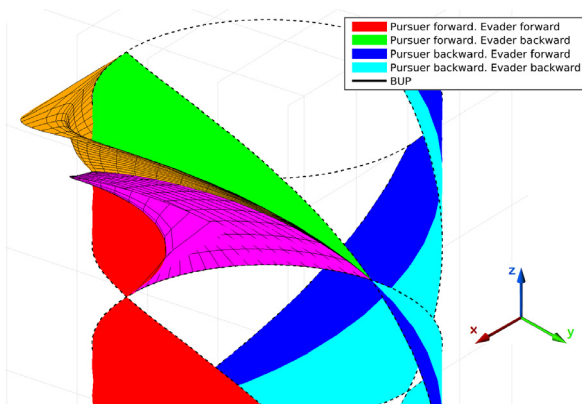


Fig. 13. The transition surfaces from PFEF+ and PFEB+ are shown in magenta and orange, respectively. The trajectories starting from PFEF+ (red) go to the magenta surface. Similar behavior occurs for the trajectories starting from PFEB+ (green); they go to the blue surface. Notice that both surfaces do not intersect. Besides, these trajectories stay inside the barrier before the first switch of controls. (For interpretation of the references to color in this figure legend, the reader is referred to the web version of this article.)

### 7.2.1. Second switch of controls

The time-optimal controls of the players correspond to saturated maximum speeds, differing only in the sign, which depends on the sign of the following functions

$$\begin{aligned}
 f_{u_1}(\tau) &= -\lambda_x(\tau)y(\tau) + \lambda_y(\tau)x(\tau) - b\lambda_y(\tau) - \lambda_\theta(\tau) \\
 f_{u_2}(\tau) &= \lambda_x(\tau)y(\tau) - \lambda_y(\tau)x(\tau) - b\lambda_y(\tau) + \lambda_\theta(\tau) \\
 f_{v_1}(\tau) &= b\lambda_x(\tau) \sin(\theta(\tau)) + b\lambda_y(\tau) \cos(\theta(\tau)) + \lambda_\theta(\tau) \\
 f_{v_2}(\tau) &= b\lambda_x(\tau) \sin(\theta(\tau)) + b\lambda_y(\tau) \cos(\theta(\tau)) - \lambda_\theta(\tau)
 \end{aligned} \tag{73}$$

where

$$\lambda_x = \sin s_1, \lambda_y = \cos s_1, \lambda_\theta = -b \cos(s_1 - s_2) \tag{74}$$

and  $(x(\tau), y(\tau), \theta(\tau))$  is the position of the evader as it travels the trajectory after the first switch of controls. We need to find whether there is a valid time  $\tau$  where the controls change their signs. A valid time is greater than  $\tau_s$  and not larger than the time allowing to cross the barrier. For the controls  $u_1$  and  $u_2$ , from a trajectory going out from PFEF+, it is possible to factorize  $\tau$ , obtaining

$$\begin{aligned}
 \tau &= \frac{b}{V^{max}}(\cot(s_1) - \cot(s_1 - s_2)) - \frac{l_c \sin(s_1 - s_2)}{V^{max} \sin(s_1)} \text{ for } u_1 \\
 \tau &= \frac{b}{V^{max}}(\cot(s_1 - s_2) + \cot(s_1)) - \frac{l_c \sin(s_1 - s_2)}{V^{max} \sin(s_1)} \text{ for } u_2
 \end{aligned} \tag{75}$$

For controls  $v_1$  and  $v_2$  we can also find a switch time

$$\begin{aligned}
 \tau &= -\frac{V^{max}}{b}(\pi k - \pi/2) + \tau_s \text{ for } v_1 \\
 \tau &= -\frac{V^{max}}{b}(s_2 - s_1 + \cos^{-1}(-\cos(s_1 - s_2)) + 2\pi k) + \tau_s \text{ for } v_2
 \end{aligned} \tag{76}$$

such that  $k$  makes the final configuration in retro-time belongs to the region of the playing space where the pursuer wins.

The existence of a second switch of controls depends on a valid value for  $\tau$ . Another issue to take into account corresponds to determine whether or not an intersection between trajectories exists before the second switch of controls.

### 7.2.2. Intersection with other trajectories

One must consider all the possibilities. The cases are the following:

- Trajectories from PFEF+ after the first switch of controls intersect with trajectories from PFEB+ before the first switch of controls. That is, find  $\tilde{\tau}$ ,  $(\hat{s}_1, \hat{s}_2) \in \text{PFEF+}$ , and  $(\tilde{s}_1, \tilde{s}_2) \in \text{PFEB+}$  that satisfy the following three equations

$$b \cot(\hat{s}_1 - \hat{s}_2) \sin(\hat{s}_2) + l_c \sin(\hat{s}_1) = \tilde{\tau} V^{max} \sin(\tilde{s}_2) + l_c \sin(\tilde{s}_1) \quad (77)$$

$$\begin{aligned} -b \cot(\hat{s}_1 - \hat{s}_2)(1 - \cos(\hat{s}_2)) + l_c \cos(\hat{s}_1) + V^{max}(\tilde{\tau} - \tau_s) \\ = \tilde{\tau} V^{max}(1 + \cos(\tilde{s}_2)) + l_c \cos(\tilde{s}_1) \end{aligned} \quad (78)$$

$$\hat{s}_2 + \frac{V^{max}}{b}(\tilde{\tau} - \tau_s) = \tilde{s}_2 \quad (79)$$

- Trajectories from PFEF+ after the first switch of controls intersect with trajectories from PFEB+ after the first switch of controls. That is, find  $\tilde{\tau}$ ,  $(\hat{s}_1, \hat{s}_2) \in \text{PFEF+}$ , and  $(\tilde{s}_1, \tilde{s}_2) \in \text{PFEB+}$  that satisfy the following three equations

$$b \cot(\hat{s}_1 - \hat{s}_2) \sin(\hat{s}_2) + l_c \sin(\hat{s}_1) = b \cot(\tilde{s}_1 - \tilde{s}_2) \sin(\tilde{s}_2) + l_c \sin(\tilde{s}_1) \quad (80)$$

$$\begin{aligned} -b \cot(\hat{s}_1 - \hat{s}_2)(1 - \cos(\hat{s}_2)) + l_c \cos(\hat{s}_1) + V^{max}(\tilde{\tau} - \tau_s) \\ = b \cot(\tilde{s}_1 - \tilde{s}_2)(1 + \cos(\tilde{s}_2)) + l_c \cos(\tilde{s}_1) + V^{max}(\tilde{\tau} - \tau_s) \end{aligned} \quad (81)$$

$$\hat{s}_2 + \frac{V^{max}}{b}(\tilde{\tau} - \tau_s) = \tilde{s}_2 - \frac{V^{max}}{b}(\tilde{\tau} - \tau_s) \quad (82)$$

- Trajectories from PFEF+ before the first switch of controls intersect with trajectories from PFEB+ after the first switch of controls. That is, find  $\tilde{\tau}$ ,  $(\hat{s}_1, \hat{s}_2) \in \text{PFEF+}$ , and  $(\tilde{s}_1, \tilde{s}_2) \in \text{PFEB+}$  that satisfy the following three equations

$$-\tilde{\tau} V^{max} \sin(\hat{s}_2) + l_c \sin(\hat{s}_1) = b \cot(\tilde{s}_1 - \tilde{s}_2) \sin(\tilde{s}_2) + l_c \sin(\tilde{s}_1) \quad (83)$$

$$\begin{aligned} \tilde{\tau} V^{max}(1 - \cos(\hat{s}_2)) + l_c \cos(\hat{s}_1) = b \cot(\tilde{s}_1 - \tilde{s}_2)(1 + \cos(\tilde{s}_2)) + l_c \cos(\tilde{s}_1) + V^{max}(\tilde{\tau} - \tau_s) \end{aligned} \quad (84)$$

$$\hat{s}_2 = \tilde{s}_2 - \frac{V^{max}}{b}(\tilde{\tau} - \tau_s) \quad (85)$$

### 7.2.3. Intersection with the barrier

We need to know what event occurs first (retro-time) either a trajectory hits the barrier or it intersects another trajectory.

To determine if the events above occur, one needs to solve trigonometric transcendental equations. For that reason, we were not able to solve it analytically. Instead, we have done a numerical analysis, where we evaluate the cases over PFEF+ and PFEB+, and the behavior of the controls of the players for each game are obtained. That analysis is presented just below.

### 7.2.4. Numerical analysis of trajectories after the first switch of controls

We started our analysis considering the behavior of trajectories and controls after the first switch. We have included a figure that shows which event happens first. The possible events we found are: (1) the trajectory hits the barrier, (2) control  $u_1$  changes its sign, (3) control  $u_2$  changes its sign and (4) control  $v_2$  changes its sign, see Fig. 14.

A particular event happens near the boundary that PFEF+ and PFEB+ share. As the retro-time progress, the controls of the players for configurations in one side of the boundary become the controls of the players for configurations in the other side, and the trajectories in both sides have a similar cost. This suggests the existence of a dispersal surface near that boundary.

In an attempt to characterize a dispersal surface, we have considered reflected configurations over the boundary that divides PFEF+ and PFEB+. Suppose that we have a configuration  $(\hat{s}_1, \hat{s}_2) \in \text{PFEF+}$ , we take the configuration  $(\tilde{s}_1, \tilde{s}_2) \in \text{PFEB+}$  that is the reflection of  $(\hat{s}_1, \hat{s}_2)$  over the segment that divides PFEF+ and PFEB+. This reflection is given by  $\tilde{s}_1 = \hat{s}_2 - \pi/2$ , and  $\tilde{s}_2 = \hat{s}_1 + \pi/2$ . Both trajectories are plotted using the same retro-time until they get close enough (a distance factor equal to  $10e - 4$ ). If they get that close then they are marked. These end points are shown in Fig. 15. A comparison between Figs. 14 and 15 show that the blue points in Fig. 15 and the yellow point in Fig. 14 are equally located.

The analysis gives some insight of the trajectories and the controls behavior after the first switch.

## 7.3. Summary

In this work, we have found three different strategies for the players when capture is achieved. In the first one, the evader starts rotating in place at maximum speed, and after some time it switches its controls ending the game translating at maximum speed. In the second one, the evader always moves following a straight line at maximum speed. In both cases, the strategy for the pursuer is translating at maximum speed. In the third case, both players start rotating in place at maximum speed. After some time, the pursuer switches its controls and it translates at maximum speed, while the evader continues rotating in place. A time later, the evader also switches its controls and it translates at maximum speed, until the capture is achieved. Our analytical results and some numerical experiments suggest that this may be the only strategies for the players in this game.

## 8. Simulations

In this section, we present some simulations of the pursuit-evasion game. We use meters ( $m$ ) as units for distance, seconds ( $s$ ) for time, and  $m/s$  for velocities. We present three cases. (1) the pursuer wins, and both players translate at maximum speed the whole game. (2)

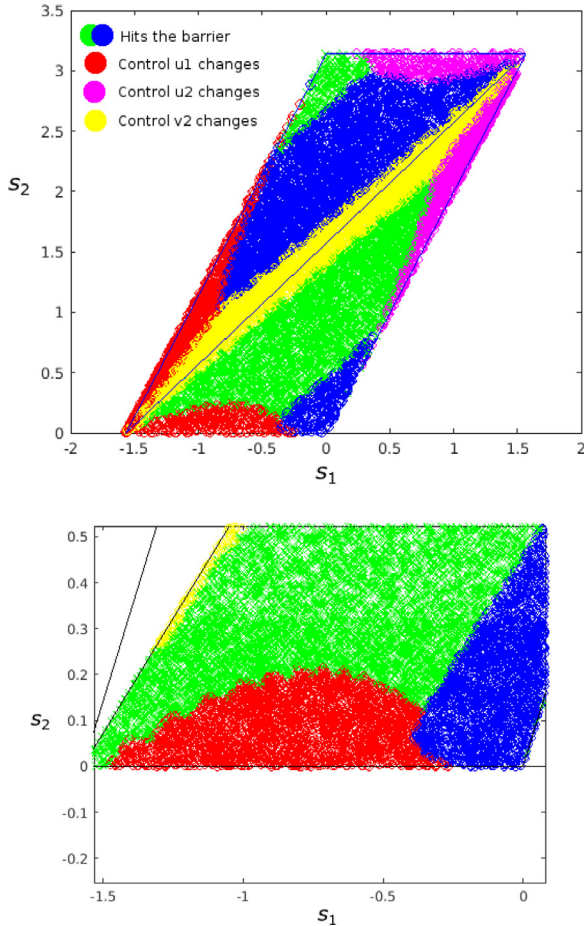


Fig. 14. This figure shows the behavior of each configuration. We took random positions at the UP and use the time-optimal retro-time controls after the first switch and until a second switch occurs, or the trajectory hits the barrier. The bottom figure is a zoom of the bottom part of the top figure.

the pursuer wins moving forward at maximum speed all the time, but the evader performs an initial rotation in place at maximal rotational speed, and after that, it moves forward at maximum translational speed. (3) the evader wins, and both players translate at maximum speed the whole game.

8.1. Both players move forward at maximum speed and the pursuer wins

In this simulation, the pursuer captures the evader while both players apply their time-optimal controls (they move forwards). The parameters for this simulation were  $l_c = 2$ ,  $b = 1.0$ ,  $V^{max} = 1.0$ . In the reduced space, the evader is initially located at  $(x_i, y_i, \theta_i) = (0.8940, 2.0897, -0.2)$ , and it is captured at  $(x_f, y_f, \theta_f) = (0, 2, -0.2)$ . Fig. 16(a) and (c) shows the initial and final configurations of the game in the reduced space. The correspond-

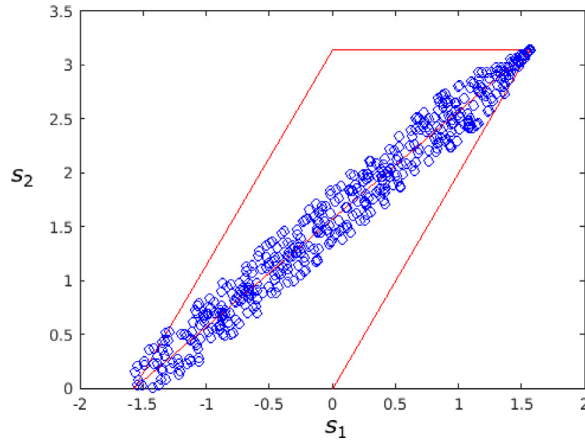
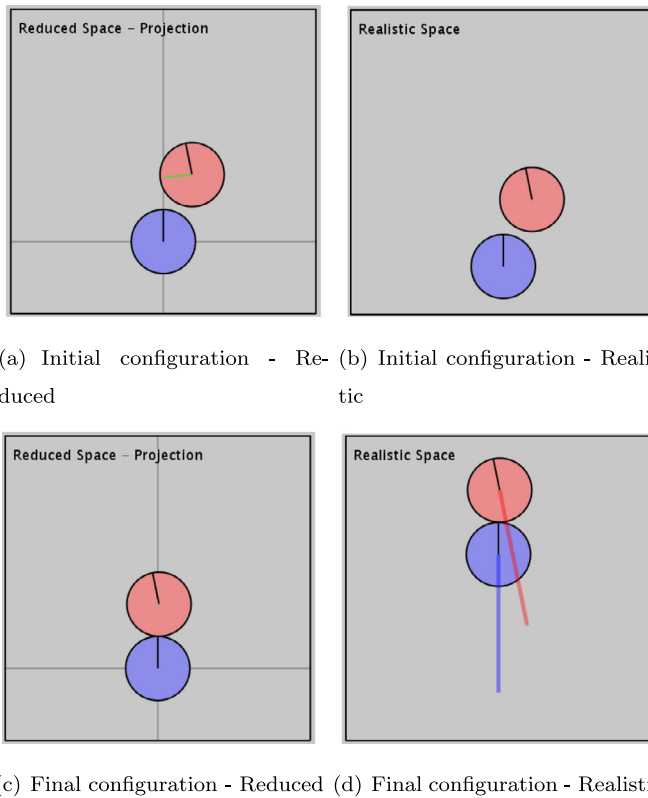


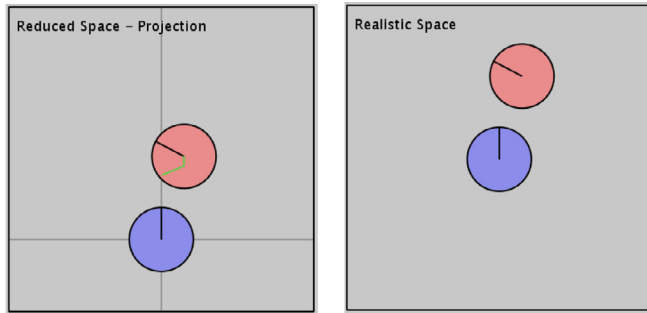
Fig. 15. This figure shows random end-configurations (at the UP) that take the trajectory near its reflection across the boundary of PFEF+ and PFEF+ using the same retro-time. Both get close enough to consider the existence of a dispersal surface.



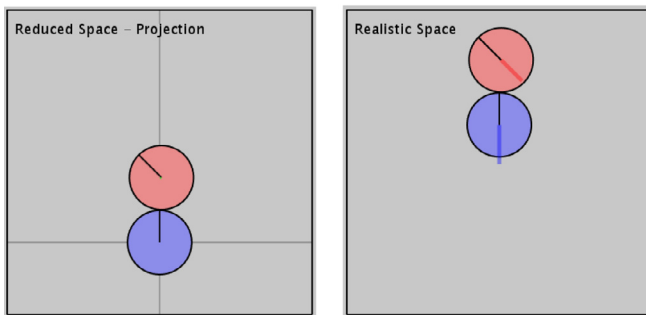
(a) Initial configuration - Reduced (b) Initial configuration - Realistic

(c) Final configuration - Reduced (d) Final configuration - Realistic

Fig. 16. The pursuer wins, and both players translate at maximum speed the whole game. The pursuer is represented like a blue disc and the evader like a red disc. The trajectories followed by the players in the realistic space are shown in (d). (For interpretation of the references to color in this figure legend, the reader is referred to the web version of this article.)



(a) Initial configuration - Reduced (b) Initial configuration - Realistic



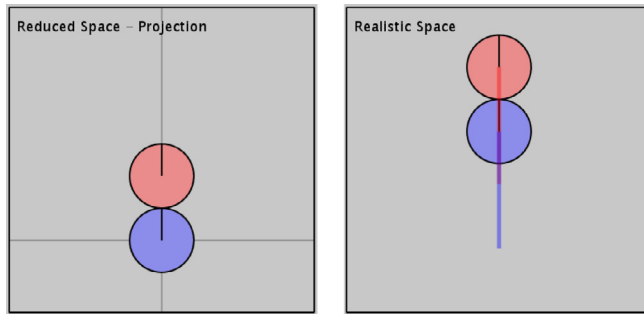
(c) Final configuration - Reduced (d) Final configuration - Realistic

Fig. 17. The pursuer wins moving forward at maximum speed all the time, but the evader performs an initial rotation in place at maximal rotational speed, and after that, it moves forward at maximum translational speed. The pursuer is represented like a blue disc and the evader like a red disc. The trajectories followed by the players in the realistic space are shown in (d). Note that the orientation of the evader at the final configuration is different from the one at the initial configuration. (For interpretation of the references to color in this figure legend, the reader is referred to the web version of this article.)

ing configurations in the realistic space are shown in Fig. 16(b) and (d), respectively. The trajectories followed by the players in the realistic space are also shown in Fig. 16(d). Note that despite both players have the same speed and move forward, capture is attained.

### 8.2. The evader initially performs a rotation in place

In this simulation, the pursuer again captures the evader, however, the time-optimal motion strategy for the evader consist of two motion primitives. First, it rotates in place at maximum rotational speed and after that, it moves forwards at maximum translational speed. The parameters for this simulation were  $l_c = 2$ ,  $b = 1.0$ ,  $V^{max} = 1.0$ . In the reduced space, the evader is initially located at  $(x_i, y_i, \theta_i) = (0.7071, 2.5929, -1.0854)$  (see Fig. 17(a)) and it is captured at  $(x_f, y_f, \theta_f) = (0, 2, \pi/4)$  (see Fig. 17(b)). The corresponding configurations in the realistic space are shown in Fig. 17(b) and (d), respectively.



(a) Final configuration - Reduced (b) Final configuration - Realistic

Fig. 18. The evader wins, and both players translate at maximum speed the whole game. The pursuer is represented like a blue disc and the evader like a red disc. The players can only keep the same distance all the time. (For interpretation of the references to color in this figure legend, the reader is referred to the web version of this article.)

### 8.3. The evader wins the game

In this simulation, the evader wins, and both players translate forwards at maximum speed the whole game. The parameters for this simulation were  $l_c = 2.0$ ,  $b = 1.0$ ,  $V^{max} = 1.0$ . In the reduced space, the evader is initially located at  $(x_i, y_i, \theta_i) = (0, 2, 0)$ . The corresponding configurations in the reduced space are shown in Fig. 18. Since both players move in the same direction, they can only keep the same distance all the time.

In the *multimedia material* of this paper, we have included a video presenting four experiments. The first experiment corresponds to the first simulation described above in this section. The second and third experiments compare the time-optimal strategy against a sub-optimal strategy for the evader yielding a smaller capture time. In the last experiment in the video, the evader wins performing a cyclic motion sliding over the barrier.

## 9. Conclusions and future work

In this work, we have addressed a pursuit–evasion problem between two identical Differential Drive Robots. The main results are:

The existence of cases where the evader wins (it avoids capture forever) is shown, which indicates that in the game addressed in this paper the barrier is closed. Furthermore, based on the initial configuration of the evader one can determine the winner of the game.

The motion primitives and time-optimal strategies for the players are found. In the realistic space, the motion primitives are straight lines and rotations in place. Some insight about the motion strategies (controls of the players) in all the region of the playing space where the pursuer wins is provided based on numerical analysis. Some simulations of the pursuit–evasion game are presented, and they show the time-optimal motion primitives of the players for cases in which either the pursuer or the evader wins, in both the reduced and the realistic space.

As future work, we want to study the case where the players do not have the same speed or radius. We are also interested in developing motion strategies where two or more pursuers cooperate to capture the evader. The motion strategies found in this work may be used as a starting point to develop such strategies.

We believe that our work can be extended to consider closed-loop policies, which are based on feedback information, making it robust to perturbations since it will be possible to correct the robot's action at each control cycle, as in [9], we left that extension as future work.

## Acknowledgments

This work was financially supported by CONACYT Consortium of Artificial Intelligence, Catedras-CONACYT project 1850 and CONACYT grant A1-S-21934.

## Appendix

In this section, we have included a list of acronyms and the general notation used in the paper.

Table 7  
List of acronyms.

|       |  |
|-------|--|
| DDR   | Differential Drive Robot   |
| OA    | Omnidirectional Agent  |
| UP    | Usable part  |
| BUP   | Boundary of the usable part  |
| SoA   | Surface of alignment   |
| PFEF+ | Pursuer translates forward, Evader translates forward, $s_2 > 0$   |
| PFEF- | Pursuer translates forward, Evader translates forward, $s_2 < 0$   |
| PFEB+ | Pursuer translates forward, Evader translates backward, $s_2 > 0$  |
| PFEB- | Pursuer translates forward, Evader translates backward, $s_2 < 0$  |
| PBEF+ | Pursuer translates backward, Evader translates forward, $s_2 > 0$  |
| PBEF- | Pursuer translates backward, Evader translates forward, $s_2 < 0$  |
| PBEB+ | Pursuer translates backward, Evader translates backward, $s_2 > 0$ |
| PBEB- | Pursuer translates backward, Evader translates backward, $s_2 < 0$ |
| TS    | Transition surface   |

Table 8  
General notation.

| Symbol                                   | Definition   |
|--|--|
| $(x_p, y_p, \theta_p)$                   | Pursuer's state in the realistic space                     |
| $(x_e, y_e, \theta_e)$                   | Evader's state in the realistic space                      |
| $v^{\max}$                               | Maximum speed  |
| $l_c$                                    | Capture distance   |
| $t_f$                                    | Capture time   |
| $(\dot{x}_p, \dot{y}_p, \dot{\theta}_p)$ | Pursuer's velocities in the realistic space                |
| $(\dot{x}_e, \dot{y}_e, \dot{\theta}_e)$ | Evader's velocities in the realistic space                 |
| $u_1, u_2$                               | Velocities of the left and the right wheel of pursuer      |
| $v_1, v_2$                               | Velocities of the left and the right wheel of evader       |
| $b$                                      | Distance between the robot's center and the wheel location |
| $\mathbf{x} = (x, y, \theta)$            | Evader's state in the reduced space                        |
| $\dot{\mathbf{x}} = f(\mathbf{x}, u, v)$ | Evader's velocity in the reduced space                     |
| $u = (u_1, u_2)$                         | Pursuer's controls   |
| $v = (v_1, v_2)$                         | Evader's controls  |

(continued on next page)

Table 8 (continued)

| Symbol   | Definition  |
|--|---|
| $H(\mathbf{x}, \lambda, u, v)$                     | Hamiltonian of the system                                     |
| $\lambda = (\lambda_x, \lambda_y, \lambda_\theta)$ | Costate variables   |
| $u^*, v^*$   | Optimal controls of the players                               |
| $\text{sgn}()$                                     | Sign function   |
| $\tau$   | Retro-time  |
| $\mathbf{x}(\tau)$                                 | Retro-time state in the reduced space                         |
| $\dot{\mathbf{x}}, \dot{\lambda}$                  | Retro-time derivative of $\mathbf{x}$ and $\lambda$           |
| $\zeta$  | Terminal surface  |
| $s_1$  | Angle between the evader’s position and the pursuer’s heading |
| $s_2$  | Angle between the heading of both players                     |
| $\tau_s^p, \tau_s^e$                               | Transition time for the pursuer and the evader                |
| $\tau_{SoA}$                                       | Time to surface of alignment                                  |

**Supplementary material**

Supplementary material associated with this article can be found, in the online version, at doi:[10.1016/j.jfranklin.2020.03.009](https://doi.org/10.1016/j.jfranklin.2020.03.009).

**References**

- [1] R. Isaacs, *Differential Games: A Mathematical Theory with Applications to Warfare and Pursuit, Control and Optimization*, John Wiley and Sons, Inc., New York, 1965.
- [2] A.W. Merz, *The homicidal chauffeur – a differential game*, Stanford University, 1971 (Phd. thesis).
- [3] A. Friedman, *Differential games*, dover, 2006,
- [4] S. Bhattacharya, S. Hutchinson, On the existence of Nash equilibrium for a two player pursuit–evasion game with visibility constraints, *Int. J. Robot Res.* 29 (7) (2010) 831–839.
- [5] W. Li, A dynamics perspective of pursuit–evasion: capturing and escaping when the pursuer runs faster than the agile evader, *IEEE Trans. Autom. Control* 62 (1) (2017) 451–457.
- [6] U. Ruiz, R. Murrieta-Cid, J.L. Marroquin, Time-optimal motion strategies for capturing an omnidirectional evader using a differential drive robot, *IEEE Trans. Robot.* 29 (5) (2013) 1180–1196.
- [7] D. Jacobo, U. Ruiz, R. Murrieta-Cid, H.M. Becerra, J.L. Marroquin, A visual feedback-based time-optimal motion policy for capturing an unpredictable evader, *Int. J. Control* 88 (4) (2015) 663–681.
- [8] U. Ruiz, R. Murrieta-Cid, A differential pursuit/evasion game of capture between an omnidirectional agent and a differential drive robot, and their winning roles, *Int. J. Control* 89 (11) (2016) 2169–2184.
- [9] V. Macias, I. Becerra, R. Murrieta-Cid, H.M. Becerra, S. Hutchinson, Image feedback based optimal control and the value of information in a differential game, *Automatica* 90 (2018) 271–285.
- [10] Jean-Paul, P. Laumond, *Robot Motion Planning and Control*, Springer-Verlag, Berlin, Heidelberg, 1998.
- [11] J. Flynn, Lion and man: the general case, *SIAM J. Control* 12 (1974) 581–597.
- [12] T. Başar, G. Olsder, *Dynamic noncooperative game theory*, in: *SIAM Series in Classics in Applied Mathematics*, 2nd ed., Philadelphia, 1999.
- [13] J. Chen, W. Zha, Z. Peng, D. Gu, Multi-player pursuit-evasion games with one superior evader, *Automatica* 71 (2016) 24–32.
- [14] L. Guibas, J.-C. Latombe, S.M. LaValle, D. Lin, R. Motwani, Visibility-based pursuit-evasion in a polygonal environment, *Int. J. Comput. Geom. Appl.* 9 (5) (1999) 471–494.
- [15] R. Vidal, O. Shakernia, H. Jin, D. Hyunchul, S. Sastry, Probabilistic pursuit-evasion games: theory, implementation, and experimental evaluation, *IEEE Trans. Robot. Autom.* 18 (5) (2002) 662–669.
- [16] R. Murrieta-Cid, T. Muppirlala, A. Sarmiento, S. Bhattacharya, S. Hutchinson, Surveillance strategies for a pursuer with finite sensor range, *Int. J. Robot Res.* 26 (3) (2007) 233–253.
- [17] B. Tovar, S.M. LaValle, Visibility-based pursuit–evasion with bounded speed, *Int. J. Robot. Res.* 27 (11–12) (2008) 1350–1360.

- [18] G. Hollinger, S. Singh, J. Djugash, A. Kehagias, Efficient multi-robot search for a moving target, *Int. J. Robot. Res.* 28 (2) (2009) 201–219.
- [19] T. Chung, G. Hollinger, V. Isler, Search and pursuit-evasion in mobile robotics: a survey, *Auton. Robot.* 31 (4) (2011) 299–316.
- [20] S.M. LaValle, H.H. González-Baños, C. Becker, J.C. Latombe, Motion strategies for maintaining visibility of a moving target, *Proceedings of the IEEE International Conference on Robotics Automation*, 1, 1997, pp. 731–736.
- [21] B. Jung, G. Sukhatme, Tracking targets using multiple robots: the effect of environment occlusion, *Auton. Robots* (12) (2002) 191–205.
- [22] T. Bandyopadhyay, M.H. Ang Jr., D. Hsu, Motion planning for 3-d target tracking among obstacles, *Int. Symp. Robot. Res.* (2007) 267–279.
- [23] J.M. O’Kane, On the value of ignorance: balancing tracking and privacy using a two-bit sensor, *Proceedings of the International Workshop Algorithmic Foundations of Robotics*, 2008, pp. 235–249.
- [24] S. Bhattacharya, S. Hutchinson, A cell decomposition approach to visibility-based pursuit evasion among obstacles, *Int. J. Robot. Res.* 30 (14) (2011) 1709–1727.
- [25] I. Becerra, R. Murrieta-Cid, R. Monroy, S. Hutchinson, J.P. Laumond, Maintaining strong mutual visibility of an evader moving over the reduced visibility graph, *Auton Robots* 40 (2) (2016) 395–423.
- [26] R. Murrieta-Cid, U. Ruiz, J.L. Marroquin, J.P. Laumond, S. Hutchinson, Tracking an omnidirectional evader with a differential drive robot, *Special issue on search and pursuit/evasion*, *Auton. Robots* 31 (4) (2011) 345–366.
- [27] G. Sun, L. Wu, Z. Kuang, Z. Ma, J. Liu, Practical tracking control of linear motor via fractional-order sliding mode, *Automatica* 94 (2018) 221–235.
- [28] N. Karnad, V. Isler, Lion and man game in the presence of a circular obstacle, *Proceedings of the IEEE International Conference on Intelligent Robots and Systems*, 2009.
- [29] V. Isler, N. Karnad, The role of information in the cop-robber game, *Theor. Comput. Sci.* 3 (399) (2008) 179–190.
- [30] A. Pierson, Z. Wang, M. Schwager, Intercepting rogue robots: an algorithm for capturing multiple evaders with multiple pursuers, *Proceedings of the IEEE International Conference on Robotics and Automation*, 2017, pp. 530–537.
- [31] G. López-Nicolás, M. Aranda, Y. Mezouar, Formation of differential-drive vehicles with field-of-view constraints for enclosing a moving target, *Proceedings of the IEEE International Conference on Robotics and Automation*, 2017, pp. 261–266.
- [32] D.J. Balkcom, M.T. Mason, Time optimal trajectories for bounded velocity differential drive vehicles, *Int. J. Robot. Res.*, 21 (3) (2002) 219–232.